

This PDF is a truncated section of the full text for preview purposes only.

Where possible the preliminary material, first chapter and list of bibliographic references used within the text have been included.

For more information on how to purchase or subscribe to this or other

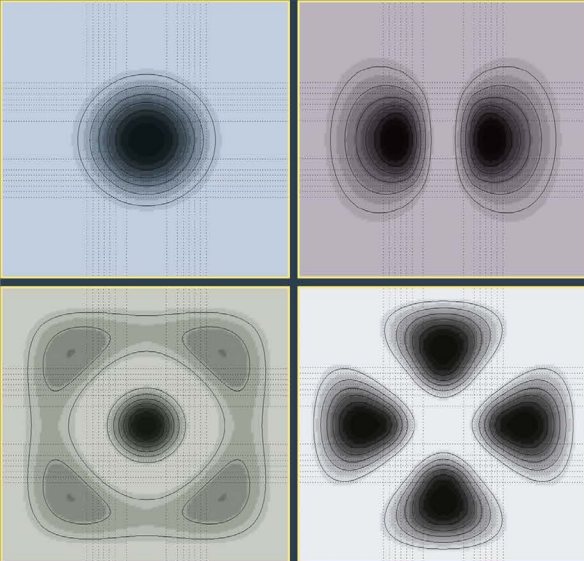
Taylor & Francis titles, please visit

<https://www.taylorfrancis.com>.

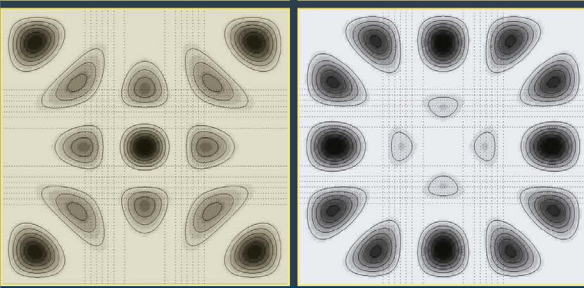
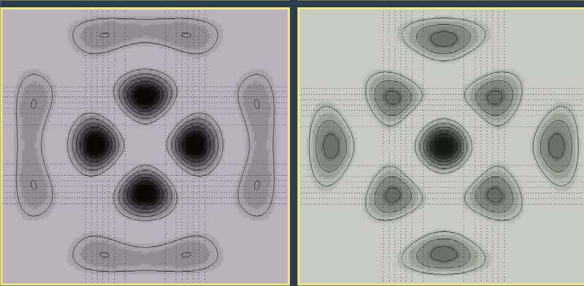
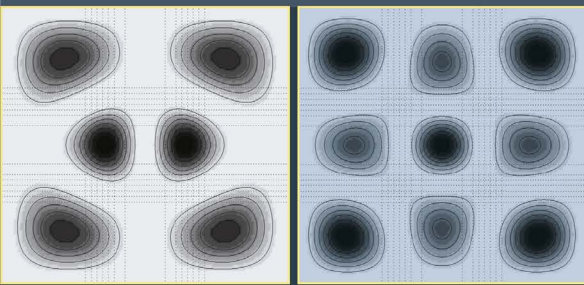
ISBN: 9781498754484 (eBook)



Taylor & Francis
Taylor & Francis Group



Diffractive Optics and Nanophotonics



Edited by V. A. Soifer



CRC Press
Taylor & Francis Group



Diffraction Optics and Nanophotonics



Taylor & Francis

Taylor & Francis Group

<http://taylorandfrancis.com>

Diffraction Optics and Nanophotonics

Edited by
V. A. Soifer



CISP



CRC Press

Taylor & Francis Group
Boca Raton London New York

CRC Press is an imprint of the
Taylor & Francis Group, an **informa** business

CRC Press
Taylor & Francis Group
6000 Broken Sound Parkway NW, Suite 300
Boca Raton, FL 33487-2742

© 2017 by CISP
CRC Press is an imprint of Taylor & Francis Group, an Informa business

No claim to original U.S. Government works

Printed on acid-free paper

International Standard Book Number-13: 978-1-4987-5447-7 (Hardback)

This book contains information obtained from authentic and highly regarded sources. Reasonable efforts have been made to publish reliable data and information, but the author and publisher cannot assume responsibility for the validity of all materials or the consequences of their use. The authors and publishers have attempted to trace the copyright holders of all material reproduced in this publication and apologize to copyright holders if permission to publish in this form has not been obtained. If any copyright material has not been acknowledged please write and let us know so we may rectify in any future reprint.

Except as permitted under U.S. Copyright Law, no part of this book may be reprinted, reproduced, transmitted, or utilized in any form by any electronic, mechanical, or other means, now known or hereafter invented, including photocopying, microfilming, and recording, or in any information storage or retrieval system, without written permission from the publishers.

For permission to photocopy or use material electronically from this work, please access www.copyright.com ([http://www.copyright.com/](http://www.copyright.com)) or contact the Copyright Clearance Center, Inc. (CCC), 222 Rosewood Drive, Danvers, MA 01923, 978-750-8400. CCC is a not-for-profit organization that provides licenses and registration for a variety of users. For organizations that have been granted a photocopy license by the CCC, a separate system of payment has been arranged.

Trademark Notice: Product or corporate names may be trademarks or registered trademarks, and are used only for identification and explanation without intent to infringe.

Visit the Taylor & Francis Web site at
<http://www.taylorandfrancis.com>

and the CRC Press Web site at
<http://www.crcpress.com>

Contents

Introduction	xii
1. The Fourier modal method and its use in plasmonics and the theory of resonant diffraction gratings	1
1.1. The Fourier modal method of solving the diffraction problems	3
1.1.1. The equation of a plane wave	3
1.1.2. The Fourier modal method for two-dimensional periodic structures	7
1.1.2.1. The geometry of the structure and formulation of the problem	8
1.1.2.2. Description of the field above and below the structure	9
1.1.2.3. The system of differential equations for the description of the field in the layer	10
1.1.2.4. Representation of the field inside the layer	21
1.1.2.5. ‘Stitching’ of the electromagnetic field at the boundaries of layers	23
1.1.2.6. The scattering matrix algorithm	26
1.1.2.7. Calculation of the field distribution	30
1.1.2.8. Intensities of the diffraction orders	31
1.1.2.9. Numerical example	33
1.1.3. The Fourier modal method for three-dimensional periodic structures	33
1.1.4. The Fourier modal method for two-dimensional non-periodic structures	40
1.1.4.1. The geometry of the structure and formulation of the problem	40
1.1.4.2. Perfectly matched absorbing layers	41
1.1.4.3. Solution of the diffraction problem	52
1.1.4.4. The energy characteristics of the reflected and transmitted light	54
1.1.4.5. Numerical example	55
1.2. Methods for calculating eigenmodes of periodic diffractive structures	56
1.2.1. Calculation of modes based on the calculation of the poles of the scattering matrix	56
1.2.1.1. Resonant representation of the scattering matrix	57
1.2.1.2. Calculation of the poles of the scattering matrix	60

1.2.1.3. Numerical examples	67
1.2.2. Calculation of events based on calculating eigenvalues of the transfer matrix	73
1.2.2.1. Calculation of modes	73
1.2.2.2. Calculation of the field distribution	75
1.2.2.3. Numerical example	78
1.3. Resonant diffraction gratings for transformation of optical pulses	78
1.3.1. The integration and differentiation of optical pulses. Wood's anomalies	79
1.3.2. Types of gratings for integration and differentiation of pulses	82
1.3.3. Fractional integration and differentiation of optical pulses. Rayleigh–Wood anomalies	84
1.3.4. Examples of calculation of pulse differentiation	86
1.3.4.1. Calculation of the grating for differentiating pulses	86
1.3.4.2. Calculation of the grating for fractional differentiation of pulses	87
1.3.5. Example of calculation of the integrating gratings	88
1.3.5.1. Calculation of the grating for the integration of pulses	88
1.3.5.2. Calculation of the grating for the fractional integration of pulses	89
1.4. Diffractive optical elements for controlling the propagation of surface plasmon–polaritons	91
1.4.1. The dispersion relation and the properties of surface plasmon–polaritons	92
1.4.1.1. Dispersion relations	92
1.4.1.2. The properties of surface plasmon–polaritons	101
1.4.1.3. Plasmonic waveguides	104
1.4.1.4. Excitation of surface plasmon–polaritons	106
1.4.2. Phase modulation of surface plasmon–polaritons by dielectric structures	107
1.4.3. Suppression of parasitic scattering of surface plasmon–polaritons	112
1.4.3.1. Theoretical analysis of matching of transverse profiles of the field of the surface plasmon–polariton and the plasmonic mode of the dielectric/dielectric/metal waveguide	112
1.4.3.2. Suppression of parasitic scattering during the passage of surface plasmon–polaritons through two-layer dielectric structures	118
1.4.4. Design of the lens for focusing the surface plasmon–polaritons	122
1.4.4.1. Integral representations of the field in the form of the spectrum of surface plasmon–polaritons	122
1.4.4.2. Diffraction lenses for focusing the surface plasmon–	

polaritons	125
1.4.4.3. The calculation of diffractive lenses for surface plasmon polaritons with parasitic scattering suppression	128
1.4.5. Calculation of reflective Bragg gratings for surface plasmon–polaritons	131
1.5. Generation of interference patterns of evanescent electromagnetic waves by means of diffraction gratings	132
1.5.1. Theoretical description of the interference patterns of evanescent diffraction orders of gratings with one-dimensional and two-dimensional periodicity	133
1.5.1.1. One-dimensional interference patterns	133
1.5.1.2. Two-dimensional interference patterns	137
1.5.2. Formation of interference patterns of evanescent electromagnetic waves in the metal–dielectric diffraction gratings	146
1.5.2.1. Generation of one-dimensional interference patterns	146
1.5.2.2. Controlling the period of one-dimensional interference patterns by changing the parameters of the incident wave	152
1.5.2.3. Generation of two-dimensional interference patterns and control of their shape by changing the parameters of the incident wave	157
1.5.3. Generation of interference patterns of evanescent electromagnetic waves in dielectric diffraction gratings	163
1.5.3.1. Generation of one-dimensional interference patterns	166
1.5.3.2. Generation of two-dimensional interference patterns	173
2. Components of photonic crystals	182
2.1 One-dimensional and two-dimensional photonic crystals	182
2.1.1 Photonic bandgaps	182
2.1.2. Diffraction of a plane wave on a photonic crystal with no defects	185
2.1.3. The propagation of light in a photonic crystal waveguide	186
2.1.4. Photonic crystal collimators	188
2.2. The two-dimensional photonic crystal gradient Mikaelian lens	189
2.2.1. The modal solution for a gradient secant medium	191
2.2.2. Photonic crystal gradient lenses	193
2.2.3. Photonic crystal lens for coupling two waveguides	198
2.3. Simulation of three-dimensional nanophotonic devices for input of radiation in a planar waveguide	212
2.3.1. The two-dimensional simulation of the input of light in a planar waveguide using a grating	213
2.3.2. Three-dimensional modelling Mikaelian photonic crystal lens for coupling two waveguides	216
2.3.3. Three-dimensional modeling of the entire nanophotonic device	218

2.4.	Photonic crystal fibres	219
2.4.1.	Calculation of modes of photonic-crystal fibres by the method of matched sinusoidal modes (MSM method)	225
2.4.2.	Method of matched sinusoidal modes in the vector case	239
2.4.3.	Krylov method for solving non-linear eigenvalue problems	246
2.4.4.	Calculation of stepped fibre modes	251
2.4.5.	Calculation of modes of photonic crystal fibres	256
2.4.6.	Calculation of modes using Fimmwave	259
3.	Sharp focusing of light with microoptics components	267
3.1.	Numerical and experimental methods for studying sharp focusing of light	267
3.1.1.	BOR-FDTD method	267
3.1.2.	Richards–Wolf vector formula	284
3.1.3.	Scanning near-field optical microscopy	291
3.2.	Axicon	292
3.2.1.	Sharp focusing of light with radial polarization using a microaxicon	293
3.2.2.	Diffractive logarithmic microaxicon	303
3.2.3.	Binary axicons with period 4, 6 and 8 μm	312
3.2.4.	Binary axicon with a period of 800 nm	327
3.3.	Fresnel zone plate	330
3.3.1.	Comparison with the Richards–Wolf formulas	331
3.3.2.	Symmetry of the intensity and power flow of the subwavelength focal spot	336
3.4.	Focusing light with gradient lenses	348
3.4.1.	Mechanism of superresolution in a planar hyperbolic secant lens	348
3.4.2.	Gradient elements of micro-optics for achieving superresolution	358
3.4.3.	Construction of an enlarged image with superresolution using planar Mikaelian lenses	373
3.4.4.	Hyperbolic secant lens with a slit for subwavelength focusing of light	387
3.4.5.	Sharp focusing of radially polarized light with a 3D hyperbolic secant lens	393
3.4.6.	Optimizing the parameters of the planar binary lens for the visible radiation range	396
3.5.	Formation of a photon nanojet by a sphere	402
3.5.1.	Numerical simulation of passage of continuous radiation through the microsphere	404
3.5.2.	Numerical simulation of passage of pulsed radiation through a microsphere	410
3.5.3.	Experiments with focusing of light by a microsphere	413

4. Introduction	421
4.1. Formation of vortex laser beams by using singular optics elements	423
4.1.1. Theoretical analysis of the diffraction of plane and Gaussian waves on the spiral phase plate	424
4.1.2. Theoretical analysis of the diffraction of plane and Gaussian waves on a spiral axicon	432
4.1.3. Numerical modeling of the diffraction of different beams on elements of singular optics	437
4.1.4. Conclusions	441
4.2. Vector representation of the field in the focal region for the vortex transmission function	443
4.2.1. Uniformly polarized beams (linear and circular polarization)	447
4.2.1.1. Linear x-polarization	447
4.2.1.2. Circular polarization	455
4.2.2. Cylindrical vector beams (radial and azimuthal polarization)	456
4.2.2.1. The radial polarization	456
4.2.2.2. The azimuthal polarization	461
4.2.3. Generalized vortex polarization	464
4.2.4. Conclusions	467
4.3. Application of axicons in high-aperture focusing systems	469
4.3.1. Adding the axicon to the lens: the paraxial scalar model	471
4.3.2. Apodization of the short-focus lens by the axicon: the non-paraxial vector model in the Debye approximation	475
4.3.3. Using vortex axicons for spatial redistribution of components of the electric field in the focal region	483
4.3.4. Conclusions	486
4.4. Control of contributions of components of the vector electric field at the focus of the high-aperture lens using binary phase structures	487
4.4.1. Maximizing the longitudinal component for linearly polarized radiation	488
4.4.2. Increasing efficiency by focusing the radially polarized radiation	494
4.4.3. Overcoming of the diffraction limit for azimuthal polarization by the transverse components of the electric field	496
4.4.4. Conclusions	496
4.5. Minimizing the size of the light or shadow focal spot with controlled growth of the side lobes	498
4.5.1. Scalar diffraction limit: theoretical analysis	499
4.5.2. Optimization of the transmission function of the focusing system	502
4.5.3. Minimization of the light spot for radially polarized radiation	503

4.5.4.	Formation of light rings of the subwavelength radius azimuthal polarization of laser radiation	509
4.5.5.	Conclusions	512
5.	Optical trapping and manipulation of micro- and nano-objects	519
5.1.	Calculation of the force acting on the micro-object by a focused laser beam	522
5.1.1.	Electromagnetic force for the three-dimensional case	522
5.1.2.	Electromagnetic force for the two-dimensional case	524
5.1.3.	Calculation of force for a plane wave	525
5.1.4.	Calculation of force for a non-paraxial Gaussian beam	528
5.1.5.	Calculation of forces for the refractive index of the object smaller than the refractive index of the medium	534
5.2.	Methods for calculating the torque acting on a micro-object by a focused laser beam	535
5.2.1.	The orbital angular momentum in cylindrical microparticles	537
5.2.2.	The results of numerical simulation of the torque	538
5.1.7.	A geometrical optics method for calculating the force acting by light on a microscopic object	544
5.1.8.	Comparison of results of calculations by geometrical optics and electromagnetic methods	549
5.2.	Rotation of micro-objects in a Bessel beam	551
5.2.1.	Rotation of micro-objects in Bessel beams	551
5.2.2.	Optical rotation using a multiorder spiral phase plate	565
5.2.3.	Rotation of microscopic objects in a vortex light ring formed by an axicon	568
5.2.4.	Optical rotation in a double light ring	569
5.2.5.	Formation of the DOE with a liquid-crystal display	572
5.2.5.	Rotation of micro-objects by means of hypergeometric beams and beams that do not have the orbital angular momentum using the spatial light modulator	575
5.2.6.	Quantitative investigation of rotation of micro-objects in light beams with an orbital angular momentum	586
5.3.	Rotating microparticles in light beams designed and formed to obtain the maximum torque	594
5.3.1.	Formation of the light beams, consisting of several light rings	594
5.3.2.	Formation of the superposition of high-order optical vortices	604
5.3.3.	Experimental formation of vortex beams superpositions	606
5.4.	Light beams specially formed for linear displacement and positioning of micro-objects	607
5.4.1.	Encoding of amplitude by the local phase jump method	608
5.4.2.	Modification of the method of encoding the amplitude for the calculation of light fields with a complex structure	611

5.4.3.	Positioning of micro-objects using focusators	612
5.4.4.	Focusators to move micro-objects along predetermined paths	619
5.4.5.	Focusators for sorting and filtering micro-objects	624
5.4.6.	Focusators to filter certain micro-objects	626
5.4.8.	The linear movement of micro-objects in superposition of two vortex beams	637
5.5.	Formation of arrays of light ‘bottles’ with the DOE	642
5.5.1.	Bessel light beams and their remarkable properties	644
5.5.2.	Multimode Bessel beams	645
5.5.3.	Formation of light ‘bottles’ through the use of composite Bessel beams of 0 th order	647
5.5.4.	Algorithm for increasing the uniformity of light traps formed on the basis of the gradient procedure	652
5.5.5.	Formation of arrays of light ‘bottles’	660
5.5.6.	Formation of arrays of hollow light beams	669
5.5.7.	Experimental formation of arrays of light ‘bottles’ with the binary DOE	675
5.5.8.	Capture of transparent micro-objects in the system of light ‘bottle’	679
5.5.9.	Capture and displacement of metallic tin microparticles with the shape close to spherical	686
5.5.10.	The deposition and positioning of micro-objects using arrays of hollow light beams	687
5.6.	The light beams generated by the DOE for non-damaging capture of biological micro-objects	688
5.6.1.	Modification of the Gaussian beam to optimize the power characteristics of the optical trap	691
5.6.2.	Measurements of the energy efficiency of the DOE forming beams–crescents	695
5.6.3.	Experiments with optical manipulation of cells of <i>Saccharomyces cerevisiae</i>	697
Conclusions		711
Index		714

Introduction

The phenomenon of diffraction, which was originally seen as a limiting factor in optics, is now a fundamental basis for the creation of a new component base and advanced information technology.

The development of diffractive optics and nanophotonics devices is based on a computer solution of direct and inverse problems of diffraction theory, based on Maxwell's equations. Among the numerical methods for solving Maxwell's equations most widely used are: the finite-difference time-domain method, the finite element method and the Fourier modal method, and also approximate methods for calculating diffraction integrals.

The book is devoted to modern achievements of diffractive optics, focused on the development of new components and devices for nanophotonics, and devices and information technologies based on them.

The first chapter describes the Fourier modal method, designed for the numerical solution of Maxwell's equations, as well as some of its applications in problems of calculation of diffractive gratings with the resonance properties and plasmon optics components.

The Fourier modal method (or rigorous-coupled wave analysis) has a wide range of applications. In the standard formulation the method is used to solve the problems of diffraction of a monochromatic plane wave on diffraction gratings. Introduction of the light beam in a plane-wave basis allows to use the method for modelling the diffraction of optical pulses. Using the so-called perfectly matched layers in combination with artificial periodization enables the method to be used efficiently to solve the problems of the diffraction of light waves by non-periodic structures. In this chapter the Fourier modal method is considered for solving the diffraction of a plane wave in the two-dimensional and three-dimensional diffractive gratings, as well as in the case of non-periodic structures. The implementation of the method is based on the numerical-stable approach, known as the scattering matrix method.

The resonance features in the spectra of periodic diffraction structures are studied using the methods developed by the authors for calculating the scattering matrix poles. These methods take into account the form of the matrix in the vicinity of the resonances associated with the excitation of eigenmodes in the lattice and, compared with the known methods, have better convergence.

The Fourier modal method and scattering matrix formalism are applied to the calculation of diffractive gratings with the resonance properties for the conversion of optical pulses. The chapter proposes a theoretical model of resonant gratings performing operations of differentiation and integration of the optical pulse envelope and the results of the calculation and research of diffractive gratings for the differentiation and integration of picosecond pulses are presented.

The non-periodic variant of the Fourier modal method is used in the problem of calculating the diffractive optical elements for controlling the propagation of surface plasmon-polaritons. The principle of operation is based on the phase modulation of surface plasmon-polaritons by dielectric steps with changing height and length and located on the surface of the metal.

The Fourier modal method is also applied to the task of calculating the diffractive gratings forming, in the near-field, interference patterns of evanescent electromagnetic waves and, in particular plasmon modes. The chapter provides a theoretical description and a number of numerical examples of calculation of the gratings forming interference patterns of evanescent electromagnetic waves and plasmon modes with a substantially subwavelength period and demonstrates the ability to control the type and period of the interference patterns of damped waves due to changes in the parameters of the incident radiation.

The practical use of the results of the first chapter includes systems for optical computing and ultra-fast optical information processing, the creation of high-performance components plasmon optics, the contact lithography systems and the systems for optical trapping and manipulation of nanoscale objects.

The second chapter deals with the nanophotonics components based on photonic crystals: the gradient planar photonic crystal (PC) lens and photonic crystal fibers. The ultra-compact nanophotonic device is described for effectively connecting two-dimensional waveguides of different widths using the PC-lens. It is shown that the PC-lens focuses the light into a small focal spot directly behind the lens whose size is substantially smaller than the scalar diffraction

limit. The simulation was performed using a finite difference solution of Maxwell's equations.

The second chapter also describes the method of calculation of optical fibres with the PC cladding. In this waveguide the light propagates within the core not due to the effect of total internal reflection from the core-cladding interface, and by reflection from a multilayer Bragg mirror formed by the system of periodically spaced holes around the core. Calculation of spatial modes in PC-fibres is based on partitioning the inhomogeneous fibre cross-section into a set of rectangular cells, each with a set of known spatial sinusoidal modes. Further cross-linking of all modes is carried out at the interfaces of all cells. The PC waveguides differ from the step and gradient waveguides by that they allow the modes to be localized within the core, that is all the modes propagate inside the core and almost do not penetrate into the cladding thus increasing the diameter of the mode localized within the core. In addition, the PC waveguides with a hollow core help to avoid chromatic dispersion in the fibre and transmit light with higher power. A short pulse of light passing through in a PC waveguide of finite size is transformed at the output to white light due to non-linear dispersion. Sections of the PC waveguides are used as filters, white light sources, and non-linear optics for second harmonic generation.

The third chapter discusses the focusing of laser radiation. The concept of the diffraction limit was established in the 19th century: $d_{\min} = \lambda/(2n)$, where λ is the wavelength of light in vacuum, n is the refractive index of the medium. The third chapter shows that using diffractive micro-optics components, focusing the light near their surface it is possible to overcome the diffraction limit. Attention is given to the sharp focusing of laser light using micro-components such as the axicon, the zone plate, the binary and gradient planar microlens, microspheres. Focusing light near the surface of the micro-components allows to overcome the diffraction limit as a result of the presence of surface waves and the influence of the refractive index of the material of the focusing element. Simulation of focusing the laser beam is carried out by the approximate Richards-Wolf vector method and the finite difference solution of Maxwell's equations.

Reducing the size of the focal spot and overcoming the diffraction limit is an urgent task in the near-field microscopy, optical micromanipulation, contact photolithography, increasing the density of recording information on an optical disc, and coupling planar waveguides of different widths.

The fourth chapter describes the focusing of singular vortex laser beams. At the point of singularity the intensity of the light field is zero, and the phase is not defined. There are abrupt phase changes in the vicinity of this point. Singularities in light fields can appear as they pass through randomly inhomogeneous and non-linear media. It is also possible to excite vortex fields in laser resonators and multimode optical fibres. The most effective method of forming the vortex laser beams is to use spiral diffractive optical elements, including spiral phase plates and spiral axicons. The fourth chapter discusses the formation of vortex beams represented as a superposition of Bessel, Laguerre–Gauss, Hermite–Gauss, etc. modes. When focusing the vortex beams attention is paid to the combination of different types of polarization and phase singularities which lead to overcoming the diffraction limit of the far-field diffraction zone.

Main applications of vortex laser beams are sharp focusing of laser light, manipulation of microscopic objects and multiplexing the channels of information transmission.

In the fifth chapter we consider the problem of optical trapping, rotation, moving, positioning of micro-objects through the use of diffractive optical elements. Micro-objects are rotated by light beams with an orbital angular momentum. Considerable attention is paid to the methods of calculating the forces acting on the micro-objects in light fields. The problem of creating the torque in micromechanical systems using light beams has a fairly long history. In a number of studies the problem of rotation is considered in conjunction with other tasks: sorting, moving, positioning, etc. It should be noted that in all the above cases the focus is primarily on the manufacturing technology of micromechanics elements and no attempts are made to improve the light beams. At the same time, the calculation and application of diffractive optical elements, forming the vortex light beams for a specific form of the micromechanical component can improve the transmission efficiency of the torque in micromechanical systems.

This chapter discusses two methods of calculating the diffractive optical elements for forming light fields with a given amplitude-phase distribution. One of them is based on calculating a focusator forming a light field with a predetermined phase gradient along the contour. Another method uses the superposition of zero-order Bessel beams to form light traps in the form of hollow beams for opaque microscopic objects. The results of experiments on optical trapping and relocation

of micro-objects are presented. The chapter examines the possibility of using light beams to move the biological micro-objects.

The book has been written by experts of the Image Processing Systems Institute, Russian Academy of Sciences. In the first chapter, [sections 1.1](#) and [1.2](#) were written by D.A. Bykov, E.A. Bezus and L.L. Doskolovich, [section 1.3](#) by D.A. Bykov, L.L. Doskolovich and V.A. Soifer, [sections 1.4](#) and [1.5](#) by E.A. Bezus and L.L. Doskolovich. The second chapter was written by V.V. Kotlyar, A.A. Kovalev, A.G. Nalimov and V.A. Soifer. The third chapter – by V.V. Kotlyar, A.A. Kovalev, A.G. Nalimov and S.S. Stafeev. The fourth chapter was written by S.N. Khonina and the fifth chapter by R.V. Skidanov, A.P. Porfir'ev and V.A. Soifer.

The Fourier modal method and its use in plasmonics and the theory of resonant diffraction gratings

This chapter describes the Fourier modal method (also called rigorous coupled-wave analysis) designed for the numerical solution of Maxwell's equations, as well as some of its applications in problems of diffractive nanophotonics.

The Fourier modal method has a wide range of applications. The formulation of the method is used for the solution of the problem of diffraction of a monochromatic plane wave on diffraction gratings. The representation of a light beam in the plane wave basis allows to use the method for the simulation of the diffraction of spatio-temporal optical signals (optical pulses). The use of the so-called perfectly matched absorbing layers in combination with artificial periodization enables the method to be used to solve the problems of the diffraction of light waves by non-periodic structures.

In [section 1.1](#) the Fourier modal method is considered in the standard formulation for solving the problem of diffraction of a plane wave on two-dimensional and three-dimensional multilayered periodic diffraction structures and for the case of non-periodic structures. The considered implementation of the method is based on a numerically stable approach, known as the scattering matrix method. The method is described in detail and was used by the authors to create original computer programs for the solution of problems of diffraction on structures of various types. The readers

can safely use the formulas given in [section 1.1](#) when creating their own programs for electromagnetic modelling.

The interaction of light with a periodic structure, in particular with metal–dielectric structures, is the subject of intense research. In such structures there is a wide range of extraordinary (resonant) optical effects, including extraordinary transmission, total absorption of incident radiation, resonant changes of the transmission and reflection coefficients, the formation of regions with a high degree of localization of energy due to interference of the evanescent and plasmon waves. These effects are usually associated with the excitation in a periodic structure of quasi-guided and plasmonic eigenmodes. The modes of the structure correspond to the poles of the scattering matrix. [Section 1.2](#) presents a number of methods proposed by the authors for calculating the poles of the scattering matrix. These methods take into account the representation of scattering matrix in the vicinity of resonances and, compared with the known techniques, have better convergence.

In [section 1.3](#) the method and the scattering matrix technique are applied to the calculation of diffraction gratings with the resonant properties to transform optical pulses. The first part of this section describes in a common approach a class of transformations of optical pulses realized by resonant diffraction gratings, and proposes a theoretical model of resonant gratings performing operations of differentiation and integration of the optical pulse envelope. The model is based on the resonant representations of the complex amplitude of the zeroth diffraction order in the vicinity of the frequencies corresponding to the waveguide resonances (Wood’s anomalies) and in the vicinity of the frequency of the Rayleigh–Wood’s anomalies associated with the emergence of propagating diffraction orders. The section also presents the results of calculations and studies of diffraction gratings to perform differentiation and integration of picosecond pulses (Wood’s anomalies), as well as the operations of fractional differentiation and integration (Rayleigh–Wood anomalies).

The possible applications of the results of this section include optical computing and ultrafast optical information processing.

In [section 1.4](#) the aperiodic Fourier modal method is used for the design of diffractive optical elements (DOE) to control the propagation of surface plasmon–polaritons (SPP). The principle of operation of the conventional DOE is based on the phase modulation of the input wave field by a diffraction microrelief of variable height.

A similar approach can be used to create optical elements for the SPP. Attention is given to the mechanisms of phase modulation of the SPP and plasmonic modes of thin metal films using dielectric ridges of variable height and fixed length (or variable height and length), located on the surface of the metal. The section also describes the method of suppressing parasitic scattering in diffraction of SPP (plasmonic modes) on a dielectric ridge, based on the use of the structure of two isotropic dielectric layers on the metal surface. This two-layer structure enables phase modulation of the SPP (plasmonic modes) while reducing the energy loss in the parasitic scattering by an order of magnitude compared to single-layer steps. The section also presents the results of calculation and research of diffractive lenses for focusing the SPP based on different phase modulation methods.

The main practical application of the results of this section is the creation of high-performance elements of plasmon optics: lens, Bragg gratings, plasmonic crystals.

In [section 1.5](#) the Fourier modal method is applied to the problem of calculating diffraction gratings which generate interference patterns of evanescent electromagnetic waves in the near field (especially of plasmonic modes). The first part of the section provides a theoretical description of the interference patterns of evanescent diffraction orders for gratings with one- and two-dimensional periodicity. This is followed by a series of numerical examples of the gratings lattices, forming interference patterns of evanescent electromagnetic waves and plasmonic modes with a substantially subwavelength period, and the ability to control the type and period of the interference patterns due to changes in the parameters of the incident radiation is demonstrated.

The practical use of the results of this section includes contact nanolithography systems and systems for optical trapping and manipulation of nanoscale objects.

1.1. The Fourier modal method of solving the diffraction problems

1.1.1. The equation of a plane wave

This subsection is auxiliary. It considers the derivation of the general equation of a plane wave in an isotropic medium used in the following description of the Fourier modal method.

We write the Maxwell equations and material equations in the Gaussian system of units:

$$\begin{cases} \nabla \times \mathbf{E} = -\frac{1}{c} \frac{\partial}{\partial t} \mathbf{B}, \\ \nabla \times \mathbf{H} = \frac{1}{c} \frac{\partial}{\partial t} \mathbf{D}, \\ \mathbf{B} = \mu \mathbf{H}, \\ \mathbf{D} = \varepsilon \mathbf{E}. \end{cases} \quad (1.1)$$

Equations (1.1) are written in the absence of charges, in this case ε is the complex permittivity. For a monochromatic field

$$\begin{aligned} \mathbf{E}(x, y, z, t) &= \mathbf{E}(x, y, z) \exp(-i\omega t), \\ \mathbf{H}(x, y, z, t) &= \mathbf{H}(x, y, z) \exp(-i\omega t), \end{aligned} \quad (1.2)$$

system (1.1) takes the form:

$$\begin{cases} \nabla \times \mathbf{E} = ik_0 \mu \mathbf{H}, \\ \nabla \times \mathbf{H} = -ik_0 \varepsilon \mathbf{E}, \end{cases} \quad (1.3)$$

wherein $k_0 = 2\pi / \lambda$, λ is the wavelength. Expanding the rotor operator we get

$$\nabla \times \mathbf{E} = \begin{bmatrix} \frac{\partial E_z}{\partial y} - \frac{\partial E_y}{\partial z} \\ \frac{\partial E_x}{\partial z} - \frac{\partial E_z}{\partial x} \\ \frac{\partial E_y}{\partial x} - \frac{\partial E_x}{\partial y} \end{bmatrix} = ik_0 \mu \begin{bmatrix} H_x \\ H_y \\ H_z \end{bmatrix}, \quad \nabla \times \mathbf{H} = \begin{bmatrix} \frac{\partial H_z}{\partial y} - \frac{\partial H_y}{\partial z} \\ \frac{\partial H_x}{\partial z} - \frac{\partial H_z}{\partial x} \\ \frac{\partial H_y}{\partial x} - \frac{\partial H_x}{\partial y} \end{bmatrix} = -ik_0 \varepsilon \begin{bmatrix} E_x \\ E_y \\ E_z \end{bmatrix}. \quad (1.4)$$

To obtain the plane wave equation we will seek the solution of (1.4) in the form

$$\Phi(x, y, z) = \Phi \exp(ik_0(\alpha x + \beta y + \gamma z)), \quad (1.5)$$

where $\Phi = [E_x \ E_y \ E_z \ H_x \ H_y \ H_z]^T$ is the column vector of the components of the field. The values α , β , γ in (1.5) define the direction of propagation of the plane wave. Substituting (1.5) into

(1.4), we obtain

$$ik_0 \begin{bmatrix} \beta E_z - \gamma E_y \\ \gamma E_x - \alpha E_z \\ \alpha E_y - \beta E_x \end{bmatrix} = ik_0 \mu \begin{bmatrix} H_x \\ H_y \\ H_z \end{bmatrix}, \quad ik_0 \begin{bmatrix} \beta H_z - \gamma H_y \\ \gamma H_x - \alpha H_z \\ \alpha H_y - \beta H_x \end{bmatrix} = -ik_0 \varepsilon \begin{bmatrix} E_x \\ E_y \\ E_z \end{bmatrix}. \quad (1.6)$$

We represent the equation (1.6) in the matrix form:

$$\begin{bmatrix} 0 & -\gamma & \beta & -\mu & 0 & 0 \\ \gamma & 0 & -\alpha & 0 & -\mu & 0 \\ -\beta & \alpha & 0 & 0 & 0 & -\mu \\ \varepsilon & 0 & 0 & 0 & -\gamma & \beta \\ 0 & \varepsilon & 0 & \gamma & 0 & -\alpha \\ 0 & 0 & \varepsilon & -\beta & \alpha & 0 \end{bmatrix} \Phi = \mathbf{A} \cdot \Phi = \mathbf{0}. \quad (1.7)$$

Direct calculation shows that the determinant of the system (1.7) has the form:

$$\det \mathbf{A} = \varepsilon \mu (\alpha^2 + \beta^2 + \gamma^2 - \varepsilon \mu)^2. \quad (1.8)$$

The sought non-trivial solution of the system (1.7) exists when the determinant (1.8) is zero. If $\mu = 1$ the determinant of (1.8) vanishes provided

$$\alpha^2 + \beta^2 + \gamma^2 = \varepsilon. \quad (1.9)$$

We write down explicitly the solution of (1.6). Under the condition (1.9) the rank of the system (1.7) is equal to four, so to write the solution the values of the amplitudes E_z and H_z are fixed. We introduce the so-called E- and H-waves. For the E-wave $E_z \neq 0$, $H_z = 0$, and for the H-wave $H_z \neq 0$, $E_z = 0$. We represent the desired solution as a superposition of the E- and H-waves in the form

$$\Phi = \frac{1}{\sqrt{\alpha^2 + \beta^2}} \begin{bmatrix} -\alpha\gamma \\ -\beta\gamma \\ \alpha^2 + \beta^2 \\ \beta\varepsilon \\ -\alpha\varepsilon \\ 0 \end{bmatrix} \frac{A_E}{\sqrt{\varepsilon}} + \frac{1}{\sqrt{\alpha^2 + \beta^2}} \begin{bmatrix} -\beta \\ \alpha \\ 0 \\ -\alpha\gamma \\ -\beta\gamma \\ \alpha^2 + \beta^2 \end{bmatrix} A_H, \quad (1.10)$$

where A_E and A_H are the the amplitudes of the E- and H-waves, respectively.

We write the components of the vector $\mathbf{p} = (\alpha, \beta, \gamma)$, representing the propagation direction of the wave, by means of the angles θ and φ of the spherical coordinate system:

$$\alpha = \sqrt{\varepsilon} \cos \varphi \sin \theta, \quad \beta = \sqrt{\varepsilon} \sin \varphi \sin \theta, \quad \gamma = \sqrt{\varepsilon} \cos \theta, \quad (1.11)$$

where θ is the angle between the vector \mathbf{p} and the axis Oz , φ is the angle between the plane of incidence and the plane xOz . For these angles the following relations are fulfilled:

$$\sqrt{\alpha^2 + \beta^2} = \sqrt{\varepsilon} \sin \theta, \quad \frac{\alpha}{\sqrt{\alpha^2 + \beta^2}} = \cos \varphi, \quad \frac{\beta}{\sqrt{\alpha^2 + \beta^2}} = \sin \varphi. \quad (1.12)$$

We write separately y - and x -components of the electric and magnetic fields:

$$\begin{aligned} \bar{\Phi} = \begin{bmatrix} E_y \\ E_x \\ H_y \\ H_x \end{bmatrix} &= \begin{bmatrix} -\cos \theta \sin \varphi \\ -\cos \theta \cos \varphi \\ -\sqrt{\varepsilon} \cos \varphi \\ \sqrt{\varepsilon} \sin \varphi \end{bmatrix} A_E + \begin{bmatrix} \cos \varphi \\ -\sin \varphi \\ -\sqrt{\varepsilon} \cos \theta \sin \varphi \\ -\sqrt{\varepsilon} \cos \theta \cos \varphi \end{bmatrix} A_H \\ &= \begin{bmatrix} \mathbf{R} & 0 \\ 0 & \mathbf{R} \end{bmatrix} \begin{bmatrix} 0 & 1 \\ -\gamma / \sqrt{\varepsilon} & 0 \\ -\sqrt{\varepsilon} & 0 \\ 0 & -\gamma \end{bmatrix} \begin{bmatrix} A_E \\ A_H \end{bmatrix}, \end{aligned} \quad (1.13)$$

where \mathbf{R} is the rotation matrix of the following form:

$$\mathbf{R} = \begin{bmatrix} \cos \varphi & \sin \varphi \\ -\sin \varphi & \cos \varphi \end{bmatrix}. \quad (1.14)$$

To describe the polarization of the wave, we introduce the angle ψ – the angle between the vector \mathbf{E} and the incidence plane. The incidence plane is the plane containing the direction of the wave propagation vector \mathbf{p} and the axis Oz . In this case

$$\begin{aligned} A_H &= A \sin \psi, \\ A_E &= A \cos \psi. \end{aligned} \quad (1.15)$$

Note that in the solution of the diffraction problem the case $\varphi = 0$ corresponds to the so-called planar diffraction. In this case the E-waves are waves with TM-polarization and H-waves the waves with TE-polarization.

Consider the time-averaged Umov–Poynting vector $\mathbf{S} = \frac{1}{2}\text{Re}(\mathbf{E} \times \mathbf{H}^*)$. We compute the z -component of the vector, which corresponds to the density of the energy flux through the plane xOy . For the E-wave

$$2S_z = \text{Re}(E_x H_y^* - E_y H_x^*) = |A_E|^2 \text{Re}(\sqrt{\varepsilon}^*) \cdot \cos\theta = |A_E|^2 \text{Re}\sqrt{\varepsilon} \cdot \cos\theta, \quad (1.16)$$

and similarly for the H-wave:

$$2S_z = \text{Re}(E_x H_y^* - E_y H_x^*) = |A_H|^2 \text{Re}(\sqrt{\varepsilon}^*) \cdot \cos\theta = |A_H|^2 \text{Re}\sqrt{\varepsilon} \cdot \cos\theta, \quad (1.17)$$

The expressions (1.16) and (1.17) describe the energy flux through the plane xOy . These expressions are important for the control of the energy conservation law in solving the problem of diffraction on diffraction structures of a lossless material.

1.1.2. The Fourier modal method for two-dimensional periodic structures

The Fourier modal method focuses on the numerical solution of Maxwell's equations for the case of periodic structures, consisting of a set of 'binary layers' [1–13]. In each layer, dielectric permittivity (magnetic permeability) of the material of the structure is independent of the variable z and the axis Oz is perpendicular to the structure. In the method the electromagnetic field in the areas above and below the structure is given as a superposition of plane waves (diffraction orders). The function of dielectric permittivity and magnetic permeability of the material in each layer of the structure are represented as segments of the Fourier series, and the components of the electromagnetic field are written as an expansion in the Fourier modes basis. The calculation of the Fourier modes is reduced to eigenvalue problems. Sequential imposition of the condition of equality of the tangential components of the electromagnetic field at the boundaries of the layers reduces the determination of the amplitudes of the reflected and transmitted diffraction orders to solving a system of linear equations [1–13].

Here the method is considered for the two-dimensional diffraction gratings (gratings with one-dimensional periodicity). In the two-dimensional case, the material properties of the structure are constant along one of the axes. The structure materials are in a general case defined by tensors of permittivity and permeability.

1.1.2.1. The geometry of the structure and formulation of the problem

Consider a diffraction grating with a period d along the axis x (Fig. 1.1). For gratings with a continuous profile (dashed line in Fig. 1.1) the method approximates the grating profile by a set of binary layers. We assume that the diffraction grating is made up of L binary layers (Fig. 1.1). The permittivity ε and permeability μ in the layers depend only on the variable x . Layer boundaries are the lines $z = d_l$, the l -th layer is located in the area $z_l < z < z_{l-1}$.

Over the considered structure in the region $z > z_0 = 0$ there is a homogeneous dielectric with a refractive index $n_U = \sqrt{\varepsilon_U}$. Under the structure there is a homogeneous dielectric with a refractive index $n_D = \sqrt{\varepsilon_D}$.

A plane monochromatic wave is incident on the top of the grating (wavelength λ , wave number $k_0 = \frac{2\pi}{\lambda}$), the direction of which is defined by the angles θ and φ in the spherical coordinate system

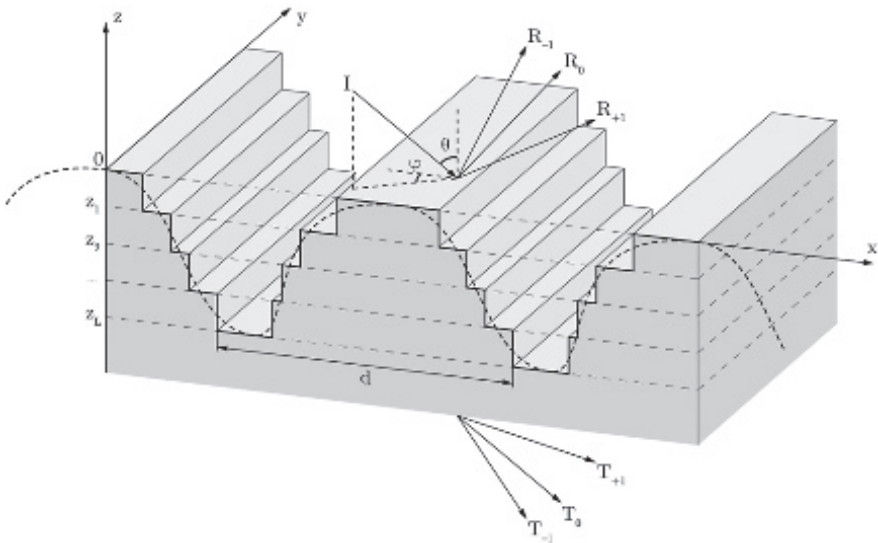


Fig. 1.1. The geometry of the problem.

(Fig. 1.1). The polarization of the wave is determined by the angle ψ between the incidence plane and the vector \mathbf{E} (see. (1.15)).

The problem of light diffraction by a periodic structure is solved by calculating the intensities or complex amplitudes of diffraction orders. The diffraction orders are the reflected and transmitted plane waves arising in the diffraction of the incident wave on the structure. There are reflected orders with amplitudes R_i , $i = 0, \pm 1, \pm 2, \dots$ and transmitted orders with amplitudes T_i , $i = 0, \pm 1, \pm 2, \dots$ (Fig. 1.1). The diffraction orders can also be divided into evanescent and propagating. The amplitude of the evanescent orders decreases exponentially away from the gratings.

1.1.2.2. Description of the field above and below the structure

The field above and below the structure is written as a superposition of plane waves (Rayleigh expansion). According to (1.5), (1.10), the plane wave is represented by a vector of six components:

$$\Phi = [E_x \quad E_y \quad E_z \quad H_x \quad H_y \quad H_z]^T. \quad (1.18)$$

The equation of the incident wave can be represented in the form

$$\Phi^{\text{inc}}(x, y, z) = \Phi^{\text{inc}}(\psi) \exp(i(k_{x,0}x + k_y y - k_{z,U,0}z)), \quad (1.19)$$

where $\Phi^{\text{inc}}(\psi)$ denotes the dependence of the incident wave on polarization (see (1.15)). The constants $k_{x,0} = k_0 n_U \sin \theta \cos \varphi$, $k_{y,0} = k_0 n_U \sin \theta \sin \varphi$, $k_{z,U,0} = \sqrt{(k_0 n_U)^2 - k_{x,0}^2 - k_y^2}$ in (1.19) are determined through the angles θ and φ defining the direction of the incident wave.

The field above the grating corresponds to the superposition of the incident wave and the reflected diffraction orders:

$$\Phi^{\text{U}}(x, y, z) = \Phi^{\text{inc}}(x, y, z) + \sum_m \Phi_m^{\text{R}}(R_m) \exp(i(k_{x,m}x + k_y y + k_{z,U,m}z)), \quad (1.20)$$

where $\Phi(R) = \Phi_E R_E + \Phi_H R_H$. Expression $\Phi(R)$ corresponds to the representation (1.10) of the reflected wave as a sum of E- and H-waves with complex amplitudes R_E and R_H respectively.

The field below the grating is expressed similarly as a superposition of transmitted waves:

$$\Phi^{\text{D}}(x, y, z) = \sum_m \Phi_m^{\text{T}}(T_m) \exp(i(k_{x,m}x + k_y y - k_{z,D,m}(z - z_L))). \quad (1.21)$$

The directions of the orders in (1.20)–(1.21) are given by propagation constants $k_{x,m}$, k_y , $k_{z,p,m}$. The propagation constants have the form

$$\begin{aligned} k_{x,m} &= k_0 \left(n_U \sin \theta \cos \varphi + m \frac{\lambda}{d} \right), \\ k_y &= k_0 n_U \sin \theta \sin \varphi, \\ k_{z,p,m} &= \sqrt{(k_0 n_p)^2 - k_{x,m}^2 - k_y^2}, \end{aligned} \quad (1.22)$$

where p is taken as ‘U’ for the reflected orders (the field above the grid) and ‘D’ – for the transmitted orders (the field under the grating). The expression for $k_{x,m}$ follows from the Floquet–Bloch theorem [14, 15]. From a mathematical point of view the form of $k_{x,m}$ provides the implementation of the so-called quasi-periodicity condition

$$\Phi^p(x+d, y, z) = \Phi^p(x, y, z) \exp(ik_{x,0}d), \quad p = \text{U, D}. \quad (1.23)$$

According to (1.23), the amplitude of the field does not change with shifts by a period. The waves with real $k_{z,p,m}$ are propagating, those with imaginary one – evanescent.

1.1.2.3. The system of differential equations for the description of the field in the layer

We turn now to the field within the particular l -th layer. For simplicity, we omit the index l .

The field in each layer is described by the Maxwell’s equations for the monochromatic field in the form

$$\begin{cases} \nabla \times \mathbf{E} = ik_0 \tilde{\boldsymbol{\mu}} \mathbf{H}, \\ \nabla \times \mathbf{H} = -ik_0 \tilde{\boldsymbol{\epsilon}} \mathbf{E}, \end{cases} \quad (1.24)$$

where $\tilde{\boldsymbol{\epsilon}}$, $\tilde{\boldsymbol{\mu}}$ are tensors in the most general case:

$$\tilde{\boldsymbol{\epsilon}} = \begin{bmatrix} \epsilon_{1,1} & \epsilon_{1,2} & \epsilon_{1,3} \\ \epsilon_{2,1} & \epsilon_{2,2} & \epsilon_{2,3} \\ \epsilon_{3,1} & \epsilon_{3,2} & \epsilon_{3,3} \end{bmatrix}, \quad \tilde{\boldsymbol{\mu}} = \begin{bmatrix} \mu_{1,1} & \mu_{1,2} & \mu_{1,3} \\ \mu_{2,1} & \mu_{2,2} & \mu_{2,3} \\ \mu_{3,1} & \mu_{3,2} & \mu_{3,3} \end{bmatrix}. \quad (1.25)$$

The tensor components depend only on the coordinate x . Expanding the rotor operator (1.24), we obtain:

$$\left\{ \begin{array}{l} \frac{\partial E_z}{\partial y} - \frac{\partial E_y}{\partial z} = ik_0(\mu_{1,1}H_x + \mu_{1,2}H_y + \mu_{1,3}H_z), \\ \frac{\partial E_x}{\partial z} - \frac{\partial E_z}{\partial x} = ik_0(\mu_{2,1}H_x + \mu_{2,2}H_y + \mu_{2,3}H_z), \\ \frac{\partial E_y}{\partial x} - \frac{\partial E_x}{\partial y} = ik_0(\mu_{3,1}H_x + \mu_{3,2}H_y + \mu_{3,3}H_z), \\ \frac{\partial H_z}{\partial y} - \frac{\partial H_y}{\partial z} = -ik_0(\varepsilon_{1,1}E_x + \varepsilon_{1,2}E_y + \varepsilon_{1,3}E_z), \\ \frac{\partial H_x}{\partial z} - \frac{\partial H_z}{\partial x} = -ik_0(\varepsilon_{2,1}E_x + \varepsilon_{2,2}E_y + \varepsilon_{2,3}E_z), \\ \frac{\partial H_y}{\partial x} - \frac{\partial H_x}{\partial y} = -ik_0(\varepsilon_{3,1}E_x + \varepsilon_{3,2}E_y + \varepsilon_{3,3}E_z). \end{array} \right. \quad (1.26)$$

We represent the components of the electric and magnetic fields in the form of Fourier series with respect to variable x :

$$\left\{ \begin{array}{l} E_x = \sum_j S_{x,j}(z) \exp(i(k_{x,j}x + k_y y)), \\ E_y = \sum_j S_{y,j}(z) \exp(i(k_{x,j}x + k_y y)), \\ E_z = \sum_j S_{z,j}(z) \exp(i(k_{x,j}x + k_y y)), \\ H_x = -i \sum_j U_{x,j}(z) \exp(i(k_{x,j}x + k_y y)), \\ H_y = -i \sum_j U_{y,j}(z) \exp(i(k_{x,j}x + k_y y)), \\ H_z = -i \sum_j U_{z,j}(z) \exp(i(k_{x,j}x + k_y y)). \end{array} \right. \quad (1.27)$$

The representations (1.27) are written with the quasi-periodicity of the field components with respect to variable x taken into account. We restrict ourselves to a finite number of terms in the expansion (1.27), corresponding to $-N \leq j \leq N$. From variables $S_{x,j}$, $S_{y,j}$, $S_{z,j}$, $U_{x,j}$, $U_{y,j}$, $U_{z,j}$, we form column vectors, \mathbf{S}_x , \mathbf{S}_y , \mathbf{S}_z , \mathbf{U}_x , \mathbf{U}_y , \mathbf{U}_z , containing $2N + 1$ elements each.

Consider the expansion of the product of two functions $\varepsilon_a(x)E_b(x,y,z)$ into the Fourier series:

$$\begin{aligned}\varepsilon_a(x)E_b(x) &= \left(\sum_m e_{a,m} \exp\left(i \frac{2\pi}{d} mx\right) \right) \cdot \left(\sum_l S_{b,l}(z) \exp\left(i(k_{x,l}x + k_y y)\right) \right) \\ &= [j=l+m] = \sum_j \left(\sum_l e_{a,j-l} S_{b,l}(z) \right) \exp\left(i(k_{x,j}x + k_y y)\right).\end{aligned}\quad (1.28)$$

Retaining a finite number of terms corresponding to $-N \leq j \leq N, -N \leq l \leq N$ in (1.28), we obtain:

$$[\varepsilon_a(x)E_b(x)] = \llbracket \varepsilon_a(x) \rrbracket \mathbf{S}_b = \llbracket \varepsilon_a(x) \rrbracket [E_b(x)], \quad (1.29)$$

where the square brackets denote the vectors composed from the Fourier coefficients of the expansion of functions $\varepsilon_a(x)E_b(x)$ and $E_b(x)$, and $\llbracket \varepsilon_a(x) \rrbracket$ is the Toeplitz matrix of the Fourier coefficients, which has the following form:

$$\mathbf{Q} = \begin{bmatrix} e_0 & e_{-1} & e_{-2} & \cdots & \cdots & e_{-2N} \\ e_1 & e_0 & e_{-1} & e_{-2} & \ddots & e_{1-2N} \\ e_2 & e_1 & e_0 & e_{-1} & \ddots & \vdots \\ \vdots & e_2 & e_1 & \ddots & \ddots & \vdots \\ \vdots & \ddots & \ddots & \ddots & \ddots & e_{-1} \\ e_{2N} & e_{2N-1} & \cdots & \cdots & e_1 & e_0 \end{bmatrix}. \quad (1.30)$$

Substituting (1.27) into (1.26) and equating coefficients of the same Fourier harmonics, we obtain:

$$\left\{ \begin{aligned} ik_0 \mathbf{K}_y \mathbf{S}_z - \frac{d\mathbf{S}_y}{dz} &= k_0 (\mathbf{M}_{1,1} \mathbf{U}_x + \mathbf{M}_{1,2} \mathbf{U}_y + \mathbf{M}_{1,3} \mathbf{U}_z), \\ \frac{d\mathbf{S}_x}{dz} - ik_0 \mathbf{K}_x \mathbf{S}_z &= k_0 (\mathbf{M}_{2,1} \mathbf{U}_x + \mathbf{M}_{2,2} \mathbf{U}_y + \mathbf{M}_{2,3} \mathbf{U}_z), \\ ik_0 \mathbf{K}_x \mathbf{S}_y - ik_0 \mathbf{K}_y \mathbf{S}_x &= k_0 (\mathbf{M}_{3,1} \mathbf{U}_x + \mathbf{M}_{3,2} \mathbf{U}_y + \mathbf{M}_{3,3} \mathbf{U}_z), \\ ik_0 \mathbf{K}_y \mathbf{U}_z - \frac{d\mathbf{U}_y}{dz} &= k_0 (\mathbf{E}_{1,1} \mathbf{S}_x + \mathbf{E}_{1,2} \mathbf{S}_y + \mathbf{E}_{1,3} \mathbf{S}_z), \\ \frac{d\mathbf{U}_x}{dz} - ik_0 \mathbf{K}_x \mathbf{U}_z &= k_0 (\mathbf{E}_{2,1} \mathbf{S}_x + \mathbf{E}_{2,2} \mathbf{S}_y + \mathbf{E}_{2,3} \mathbf{S}_z), \\ ik_0 \mathbf{K}_x \mathbf{U}_y - ik_0 \mathbf{K}_y \mathbf{U}_x &= k_0 (\mathbf{E}_{3,1} \mathbf{S}_x + \mathbf{E}_{3,2} \mathbf{S}_y + \mathbf{E}_{3,3} \mathbf{S}_z), \end{aligned} \right. \quad (1.31)$$

where $\mathbf{K}_x = \text{diag}_j \frac{k_{x,j}}{k_0}$, $\mathbf{K}_y = \text{diag}_j \frac{k_{y,j}}{k_0}$ – diagonal matrices, $\mathbf{E}_{i,j} = \llbracket \varepsilon_{i,j} \rrbracket$ and $\mathbf{M}_{i,j} = \llbracket \mu_{i,j} \rrbracket$ are the Toeplitz matrices of the form (1.30), made up of the expansion coefficients in the Fourier series $\varepsilon_{i,j}(x)$ and $\mu_{i,j}(x)$.

We perform a change of variables $z' = k_0 z$ and transform the system (1.31) to the form:

$$\left\{ \begin{array}{l} -\frac{d\mathbf{S}_y}{dz'} = \mathbf{M}_{1,1}\mathbf{U}_x + \mathbf{M}_{1,2}\mathbf{U}_y + \mathbf{M}_{1,3}\mathbf{U}_z - i\mathbf{K}_y\mathbf{S}_z, \\ -\frac{d\mathbf{S}_x}{dz'} = -\mathbf{M}_{2,1}\mathbf{U}_x - \mathbf{M}_{2,2}\mathbf{U}_y - \mathbf{M}_{2,3}\mathbf{U}_z - i\mathbf{K}_x\mathbf{S}_z, \\ \frac{d\mathbf{U}_y}{dz'} = \mathbf{E}_{1,1}\mathbf{S}_x + \mathbf{E}_{1,2}\mathbf{S}_y + \mathbf{E}_{1,3}\mathbf{S}_z - i\mathbf{K}_y\mathbf{U}_z, \\ -\frac{d\mathbf{U}_x}{dz'} = -\mathbf{E}_{2,1}\mathbf{S}_x - \mathbf{E}_{2,2}\mathbf{S}_y - \mathbf{E}_{2,3}\mathbf{S}_z - i\mathbf{K}_x\mathbf{U}_z, \\ \mathbf{E}_{3,3}\mathbf{S}_z = i\mathbf{K}_x\mathbf{U}_y - i\mathbf{K}_y\mathbf{U}_x - \mathbf{E}_{3,1}\mathbf{S}_x - \mathbf{E}_{3,2}\mathbf{S}_y, \\ \mathbf{M}_{3,3}\mathbf{U}_z = i\mathbf{K}_x\mathbf{S}_y - i\mathbf{K}_y\mathbf{S}_x - \mathbf{M}_{3,1}\mathbf{U}_x - \mathbf{M}_{3,2}\mathbf{U}_y. \end{array} \right. \quad (1.32)$$

We rewrite the first four equations of the system in matrix form:

$$\frac{d}{dz'} \begin{bmatrix} \mathbf{S}_y \\ \mathbf{S}_x \\ \mathbf{U}_y \\ \mathbf{U}_x \end{bmatrix} = \mathbf{Y} \begin{bmatrix} \mathbf{S}_y \\ \mathbf{S}_x \\ \mathbf{U}_y \\ \mathbf{U}_x \end{bmatrix} - \begin{bmatrix} -i\mathbf{K}_y & \mathbf{M}_{1,3} \\ -i\mathbf{K}_x & -\mathbf{M}_{2,3} \\ \mathbf{E}_{1,3} & -i\mathbf{K}_y \\ -\mathbf{E}_{2,3} & -i\mathbf{K}_x \end{bmatrix} \begin{bmatrix} \mathbf{S}_z \\ \mathbf{U}_z \end{bmatrix}, \quad (1.33)$$

where

$$\mathbf{Y} = - \begin{bmatrix} \mathbf{0} & \mathbf{0} & \mathbf{M}_{1,2} & \mathbf{M}_{1,1} \\ \mathbf{0} & \mathbf{0} & -\mathbf{M}_{2,2} & -\mathbf{M}_{2,1} \\ \mathbf{E}_{1,2} & \mathbf{E}_{1,1} & \mathbf{0} & \mathbf{0} \\ -\mathbf{E}_{2,2} & -\mathbf{E}_{2,1} & \mathbf{0} & \mathbf{0} \end{bmatrix}. \quad (1.34)$$

From the last two equations of (1.32) we express \mathbf{S}_z and \mathbf{U}_z and substitute the resulting expressions into (1.33). As a result, we obtain

a system of linear differential equations with respect to x - and y -Fourier components of the fields:

where

$$\frac{d}{dz'} \begin{bmatrix} \mathbf{S}_y \\ \mathbf{S}_x \\ \mathbf{U}_y \\ \mathbf{U}_x \end{bmatrix} = \mathbf{A} \begin{bmatrix} \mathbf{S}_y \\ \mathbf{S}_x \\ \mathbf{U}_y \\ \mathbf{U}_x \end{bmatrix}, \quad (1.35)$$

where

$$\mathbf{A} = \mathbf{Y} - \begin{bmatrix} i\mathbf{K}_y & -\mathbf{M}_{1,3} \\ i\mathbf{K}_x & \mathbf{M}_{2,3} \\ -\mathbf{E}_{1,3} & i\mathbf{K}_y \\ \mathbf{E}_{2,3} & i\mathbf{K}_x \end{bmatrix} \begin{bmatrix} \mathbf{E}_{3,3}^{-1} & \mathbf{0} \\ \mathbf{0} & \mathbf{M}_{3,3}^{-1} \end{bmatrix} \begin{bmatrix} \mathbf{E}_{3,2} & \mathbf{E}_{3,1} & -i\mathbf{K}_x & i\mathbf{K}_y \\ -i\mathbf{K}_x & i\mathbf{K}_y & \mathbf{M}_{3,2} & \mathbf{M}_{3,1} \end{bmatrix}. \quad (1.36)$$

Thus, we have obtained a system of linear differential equations of the first order for the vectors \mathbf{S}_x , \mathbf{S}_y , \mathbf{U}_x , \mathbf{U}_y . Note that the matrix \mathbf{A} has the dimensions $4(2N+1) \times 4(2N+1)$.

Correct rules of the Fourier expansion of the product of functions

The derivation of the system of differential equations (1.35) was based on the representation in (1.26) of the component of electromagnetic fields and of the components of permittivity and permeability tensors in the form of segments of the Fourier series. The representation of the products of the functions in (1.26) by the Fourier series has its own peculiarities. The used formulas (1.28)–(1.30) have limited applicability.

Consider two periodic functions

$$f(x) = \sum_m f_m \exp(iKmx), \quad g(x) = \sum_m g_m \exp(iKmx), \quad K = \frac{2\pi}{d} \quad (1.37)$$

and the expansion of their product into the Fourier series

$$h(x) = f(x)g(x) = \sum_m h_m \exp(iKmx). \quad (1.38)$$

The Fourier coefficients of the product are the values

$$h_j = \sum_{m=-N}^N f_{j-m} g_m \quad (1.39)$$

obtained by direct multiplication of the series (1.37), (1.38). Equation (1.39) for calculating the Fourier coefficients is called the Laurent rule. In matrix notation (1.39) can be represented as [5]

$$[h] = [[f]][g], \quad (1.40)$$

where, as in (1.29), the square brackets denote the vectors composed from the Fourier coefficients of the expansion of the functions, and $[[f]]$ is the Toeplitz matrix of the Fourier coefficients.

As was shown in [5, 6], the use of formula (1.40) is correct if there is no value x for which the functions $f(x)$ and $g(x)$ show a discontinuity at the same time. Using the Laurent rule (1.40) for the product of the functions having identical points of discontinuity leads to poor convergence of the Fourier series at the points of discontinuity.

If the functions $f(x)$ and $g(x)$ are discontinuous at the same time, but the function $h(x) = f(x)g(x)$ is continuous, it is correct to use the so-called inverse Laurent rules [5]:

$$[h] = \left[\left[\frac{1}{f} \right] \right]^{-1} [g]. \quad (1.41)$$

In the products $\mu_{i,1}(x) \cdot H_x(x, y, z)$ and $\varepsilon_{i,1}(x) \cdot E_x(x, y, z)$ in (1.26), both expanded functions have discontinuities at the same points x , corresponding to vertical interfaces of the media in the layers. Accordingly, it is erroneous to use the Laurent rule (1.28)–(1.30) when writing (1.31). Errors in the use of the Laurent rule are significant when working with diffraction gratings of conductive materials. In particular, the erroneous use of the Laurent rule leads to slow convergence of the solutions for binary metal gratings in the case of TM-polarization [5–10]. In this case we define the convergence as the stabilization of the results of the calculation of the amplitudes of diffraction orders with increasing number of the Fourier harmonics N in the components of the field (1.27).

Continuous components at the vertical boundaries between the media are the tangential components E_y , E_z , H_y , H_z and the normal components of the electric displacement and magnetic induction D_x , B_x . We express discontinuous components E_x , H_x through the continuous field components

$$E_x = \frac{1}{\varepsilon_{11}} D_x - \frac{\varepsilon_{12}}{\varepsilon_{11}} E_y - \frac{\varepsilon_{13}}{\varepsilon_{11}} E_z, \quad (1.42)$$

$$H_x = \frac{1}{\mu_{11}} B_x - \frac{\mu_{12}}{\mu_{11}} H_y - \frac{\mu_{13}}{\mu_{11}} H_z$$

and substitute into Maxwell's equations (1.26). The result is:

$$\left\{ \begin{array}{l} \frac{\partial E_z}{\partial y} - \frac{\partial E_y}{\partial z} = ik_0 B_x, \\ \frac{\partial E_x}{\partial z} - \frac{\partial E_z}{\partial x} = ik_0 \left(\frac{\alpha_{2,1}}{\alpha_{1,1}} B_x + \left(\alpha_{2,2} - \alpha_{2,1} \frac{\alpha_{1,2}}{\alpha_{1,1}} \right) H_y + \left(\alpha_{2,3} - \alpha_{2,1} \frac{\alpha_{1,3}}{\alpha_{1,1}} \right) H_z \right), \\ \frac{\partial E_y}{\partial x} - \frac{\partial E_x}{\partial y} = ik_0 \left(\frac{\alpha_{3,1}}{\alpha_{1,1}} B_x + \left(\alpha_{3,2} - \alpha_{3,1} \frac{\alpha_{1,2}}{\alpha_{1,1}} \right) H_y + \left(\alpha_{3,3} - \alpha_{3,1} \frac{\alpha_{1,3}}{\alpha_{1,1}} \right) H_z \right), \\ \frac{\partial H_z}{\partial y} - \frac{\partial H_y}{\partial z} = -ik_0 D_x, \\ \frac{\partial H_x}{\partial z} - \frac{\partial H_z}{\partial x} = -ik_0 \left(\frac{\varepsilon_{2,1}}{\varepsilon_{1,1}} D_x + \left(\varepsilon_{2,2} - \varepsilon_{2,1} \frac{\varepsilon_{1,2}}{\varepsilon_{1,1}} \right) E_y + \left(\varepsilon_{2,3} - \varepsilon_{2,1} \frac{\varepsilon_{1,3}}{\varepsilon_{1,1}} \right) E_z \right), \\ \frac{\partial H_y}{\partial x} - \frac{\partial H_x}{\partial y} = -ik_0 \left(\frac{\varepsilon_{3,1}}{\varepsilon_{1,1}} D_x + \left(\varepsilon_{3,2} - \varepsilon_{3,1} \frac{\varepsilon_{1,2}}{\varepsilon_{1,1}} \right) E_y + \left(\varepsilon_{3,3} - \varepsilon_{3,1} \frac{\varepsilon_{1,3}}{\varepsilon_{1,1}} \right) E_z \right). \end{array} \right. \quad (1.43)$$

Equations (1.43) do not contain products of functions simultaneously suffering a discontinuity. Therefore, in the transition to the space–frequency domain, we can use the direct Laurent rule (1.29), (1.30). According to (1.42), the vectors of the Fourier coefficients of the functions D_x , B_x have the form

$$\begin{aligned}
[D_x] &= \left[\frac{1}{\varepsilon_{11}} \right]^{-1} \left([E_x] + \left[\frac{\varepsilon_{12}}{\varepsilon_{11}} \right] [E_y] + \left[\frac{\varepsilon_{13}}{\varepsilon_{11}} \right] [E_z] \right), \\
[B_x] &= \left[\frac{1}{\mu_{11}} \right]^{-1} \left([H_x] + \left[\frac{\mu_{12}}{\mu_{11}} \right] [H_y] + \left[\frac{\mu_{13}}{\mu_{11}} \right] [H_z] \right).
\end{aligned} \tag{1.44}$$

Performing in (1.43) the transition to the space–frequency domain and transforming the result, we also obtain the system of differential equations (1.35)–(1.34) where the matrices $\mathbf{M}_{i,j}$ and $\mathbf{E}_{i,j}$ have the form

$$\begin{aligned}
\mathbf{M}_{1,1} &= \left[\frac{1}{\alpha_{11}} \right]^{-1}, \quad \mathbf{M}_{1,2} = \left[\frac{1}{\alpha_{11}} \right]^{-1} \left[\frac{\alpha_{12}}{\alpha_{11}} \right], \quad \mathbf{M}_{1,3} = \left[\frac{1}{\alpha_{11}} \right]^{-1} \left[\frac{\alpha_{13}}{\alpha_{11}} \right], \\
\mathbf{M}_{2,1} &= \left[\frac{\alpha_{21}}{\alpha_{11}} \right] \left[\frac{1}{\alpha_{11}} \right]^{-1}, \quad \mathbf{M}_{2,2} = \left[\alpha_{22} - \frac{\alpha_{12}\alpha_{21}}{\alpha_{11}} \right] + \left[\frac{\alpha_{21}}{\alpha_{11}} \right] \left[\frac{1}{\alpha_{11}} \right]^{-1} \left[\frac{\alpha_{12}}{\alpha_{11}} \right], \\
\mathbf{M}_{2,3} &= \left[\alpha_{23} - \frac{\alpha_{13}\alpha_{21}}{\alpha_{11}} \right] + \left[\frac{\alpha_{21}}{\alpha_{11}} \right] \left[\frac{1}{\alpha_{11}} \right]^{-1} \left[\frac{\alpha_{13}}{\alpha_{11}} \right], \\
\mathbf{M}_{3,1} &= \left[\frac{\alpha_{31}}{\alpha_{11}} \right] \left[\frac{1}{\alpha_{11}} \right]^{-1}, \quad \mathbf{M}_{3,2} = \left[\alpha_{32} - \frac{\alpha_{31}\alpha_{12}}{\alpha_{11}} \right] + \left[\frac{\alpha_{31}}{\mu_{11}} \right] \left[\frac{1}{\mu_{11}} \right]^{-1} \left[\frac{\mu_{12}}{\mu_{11}} \right], \\
\mathbf{M}_{3,3} &= \left[\mu_{33} - \frac{\mu_{31}\mu_{13}}{\mu_{11}} \right] + \left[\frac{\mu_{31}}{\mu_{11}} \right] \left[\frac{1}{\mu_{11}} \right]^{-1} \left[\frac{\mu_{13}}{\mu_{11}} \right], \\
\mathbf{E}_{1,1} &= \left[\frac{1}{\varepsilon_{11}} \right]^{-1}, \quad \mathbf{E}_{1,2} = \left[\frac{1}{\varepsilon_{11}} \right]^{-1} \left[\frac{\varepsilon_{12}}{\varepsilon_{11}} \right], \quad \mathbf{E}_{1,3} = \left[\frac{1}{\varepsilon_{11}} \right]^{-1} \left[\frac{\varepsilon_{13}}{\varepsilon_{11}} \right], \\
\mathbf{E}_{2,1} &= \left[\frac{\varepsilon_{21}}{\varepsilon_{11}} \right] \left[\frac{1}{\varepsilon_{11}} \right]^{-1}, \quad \mathbf{E}_{2,2} = \left[\varepsilon_{22} - \frac{\varepsilon_{12}\varepsilon_{21}}{\varepsilon_{11}} \right] + \left[\frac{\varepsilon_{21}}{\varepsilon_{11}} \right] \left[\frac{1}{\varepsilon_{11}} \right]^{-1} \left[\frac{\varepsilon_{12}}{\varepsilon_{11}} \right], \\
\mathbf{E}_{2,3} &= \left[\varepsilon_{23} - \frac{\varepsilon_{13}\varepsilon_{21}}{\varepsilon_{11}} \right] + \left[\frac{\varepsilon_{21}}{\varepsilon_{11}} \right] \left[\frac{1}{\varepsilon_{11}} \right]^{-1} \left[\frac{\varepsilon_{13}}{\varepsilon_{11}} \right], \\
\mathbf{E}_{3,1} &= \left[\frac{\varepsilon_{31}}{\varepsilon_{11}} \right] \left[\frac{1}{\varepsilon_{11}} \right]^{-1}, \quad \mathbf{E}_{3,2} = \left[\varepsilon_{32} - \frac{\varepsilon_{31}\varepsilon_{12}}{\varepsilon_{11}} \right] + \left[\frac{\varepsilon_{31}}{\varepsilon_{11}} \right] \left[\frac{1}{\varepsilon_{11}} \right]^{-1} \left[\frac{\varepsilon_{12}}{\varepsilon_{11}} \right], \\
\mathbf{E}_{3,3} &= \left[\varepsilon_{33} - \frac{\varepsilon_{31}\varepsilon_{13}}{\varepsilon_{11}} \right] + \left[\frac{\varepsilon_{31}}{\varepsilon_{11}} \right] \left[\frac{1}{\varepsilon_{11}} \right]^{-1} \left[\frac{\varepsilon_{13}}{\varepsilon_{11}} \right].
\end{aligned} \tag{1.45}$$

The system of differential equations (1.35) with the matrices $\mathbf{M}_{i,j}$, $\mathbf{E}_{i,j}$ in the form (1.45) will be called a system, obtained using the correct rules of the Fourier expansions of the product of the functions.

The form of the matrix of the system for different permittivity tensors

We consider some special kinds of tensors of permittivity and permeability and the corresponding matrices of the system of differential equations (1.35). The systems of differential equations are presented for the case of correct rules of the Fourier expansions.

Consider the case of an isotropic material. For this material, $\mu = 1$ and ε is a scalar. In this case, the matrices $\mathbf{E}_{i,j}$, $\mathbf{M}_{i,j}$ take the following form:

$$\begin{aligned} \mathbf{E}_{1,1} &= \mathbf{E}^* = \left[\left[\frac{1}{\varepsilon} \right] \right]^{-1}, \quad \mathbf{E}_{2,2} = \mathbf{E}_{3,3} = \mathbf{E} = \llbracket \varepsilon \rrbracket, \\ \mathbf{E}_{1,2} &= \mathbf{E}_{1,3} = \mathbf{E}_{2,1} = \mathbf{E}_{2,3} = \mathbf{E}_{3,1} = \mathbf{E}_{3,2} = \mathbf{0}, \\ \mathbf{M}_{1,1} &= \mathbf{M}_{2,2} = \mathbf{M}_{3,3} = \mathbf{I}, \\ \mathbf{M}_{1,2} &= \mathbf{M}_{1,3} = \mathbf{M}_{2,1} = \mathbf{M}_{2,3} = \mathbf{M}_{3,1} = \mathbf{M}_{3,2} = \mathbf{0}, \end{aligned} \quad (1.46)$$

where \mathbf{I} is the identity matrix with the dimensions $(2N+1) \times (2N+1)$. Substituting (1.46) into (1.36)–(1.34), we obtain the matrix of the system of differential equations in the form

$$\mathbf{A} = - \begin{bmatrix} \mathbf{0} & \mathbf{0} & \mathbf{K}_y \mathbf{E}^{-1} \mathbf{K}_x & \mathbf{I} - \mathbf{K}_y \mathbf{E}^{-1} \mathbf{K}_y \\ \mathbf{0} & \mathbf{0} & \mathbf{K}_x \mathbf{E}^{-1} \mathbf{K}_x - \mathbf{I} & -\mathbf{K}_x \mathbf{E}^{-1} \mathbf{K}_y \\ \mathbf{K}_y \mathbf{K}_x & \mathbf{E}^* - \mathbf{K}_y^2 & \mathbf{0} & \mathbf{0} \\ \mathbf{K}_x^2 - \mathbf{E} & -\mathbf{K}_x \mathbf{K}_y & \mathbf{0} & \mathbf{0} \end{bmatrix}. \quad (1.47)$$

Consider the case of a planar incidence when $k_y = 0$ ($\varphi = 0$) in (1.22) and the direction vector of the incident wave lies in the plane xOz . In this case, $\mathbf{K}_y = \mathbf{0}$ (1.47) and the system of differential equations (1.35) splits into two independent systems

$$\begin{aligned} \frac{d}{dz'} \begin{bmatrix} \mathbf{S}_y \\ \mathbf{U}_x \end{bmatrix} &= \mathbf{A}^{\text{TE}} \begin{bmatrix} \mathbf{S}_y \\ \mathbf{U}_x \end{bmatrix}, \quad \mathbf{A}^{\text{TE}} = - \begin{bmatrix} \mathbf{0} & \mathbf{I} \\ \mathbf{K}_x^2 - \mathbf{E} & \mathbf{0} \end{bmatrix}, \\ \frac{d}{dz'} \begin{bmatrix} \mathbf{U}_y \\ \mathbf{S}_x \end{bmatrix} &= \mathbf{A}^{\text{TM}} \begin{bmatrix} \mathbf{U}_y \\ \mathbf{S}_x \end{bmatrix}, \quad \mathbf{A}^{\text{TM}} = - \begin{bmatrix} \mathbf{0} & \mathbf{E}^* \\ \mathbf{K}_x \mathbf{E}^{-1} \mathbf{K}_x - \mathbf{I} & \mathbf{0} \end{bmatrix}. \end{aligned} \quad (1.48)$$

This result in the case of a planar incidence reduces the solution of the problem of diffraction to two independent problems of diffraction of the waves with TM- and TE-polarization.

Currently, there is considerable interest in the structures comprising layers of a magnetic material. In such structures the optical properties of the materials can be modified by an external magnetic field. This allows to effectively control the amplitude and phase of the diffraction orders with the help of an external magnetic field. For magnetic materials the dielectric constant is given by the tensor [16, 17]:

$$\tilde{\varepsilon} = \begin{bmatrix} \varepsilon & ig \cos \theta_M & -ig \sin \theta_M \sin \varphi_M \\ -ig \cos \theta_M & \varepsilon & ig \sin \theta_M \cos \varphi_M \\ ig \sin \theta_M \sin \varphi_M & -ig \sin \theta_M \cos \varphi_M & \varepsilon \end{bmatrix}, \quad (1.49)$$

where ε is the main dielectric constant of the medium, g is the modulus of the gyration vector of the medium proportional to the magnetization [16, 17], θ_M and φ_M are the spherical coordinates, describing the direction of the magnetization vector. In the optical frequency range $\mu = 1$.

We consider three basic cases corresponding to the direction of the magnetization vector along the three coordinate axes.

For the *polar geometry of magnetization* (magnetization vector is perpendicular to the plane of the layers of the structure and directed along the axis Oz) $\theta_M = 0$ and the tensor (1.49) takes the form:

$$\tilde{\varepsilon} = \begin{bmatrix} \varepsilon & ig & 0 \\ -ig & \varepsilon & 0 \\ 0 & 0 & \varepsilon \end{bmatrix}. \quad (1.50)$$

In this case

$$\mathbf{A} = - \begin{bmatrix} \mathbf{0} & \mathbf{0} & \mathbf{K}_y \mathbf{E}^{-1} \mathbf{K}_x & \mathbf{I} - \mathbf{K}_y \mathbf{E}^{-1} \mathbf{K}_y \\ \mathbf{0} & \mathbf{0} & \mathbf{K}_x \mathbf{E}^{-1} \mathbf{K}_x - \mathbf{I} & -\mathbf{K}_x \mathbf{E}^{-1} \mathbf{K}_y \\ i \mathbf{E}^* \mathbf{H} + \mathbf{K}_y \mathbf{K}_x & \mathbf{E}^* - \mathbf{K}_y^2 & \mathbf{0} & \mathbf{0} \\ \mathbf{K}_x^2 - \mathbf{E}_2 & i \mathbf{H} \mathbf{E}^* - \mathbf{K}_x \mathbf{K}_y & \mathbf{0} & \mathbf{0} \end{bmatrix}, \quad (1.51)$$

where

$$\mathbf{E}^* = \left[\left[\frac{1}{\varepsilon} \right] \right]^{-1}, \mathbf{E} = [\varepsilon], \mathbf{H} = \left[\left[\frac{\mathbf{g}}{\varepsilon} \right] \right], \mathbf{E}_2 = \left[\left[\varepsilon - \frac{\mathbf{g}^2}{\varepsilon} \right] \right] + \mathbf{H}\mathbf{E}^*\mathbf{H}$$

In the case of the meridional geometry of magnetization (the magnetization vector is parallel to the plane of the layers and directed along the axis Ox) $\theta_M = \frac{\pi}{2}$, $\varphi_M = 0$ and the tensor (1.49) takes the form

$$\vec{\varepsilon} = \begin{bmatrix} \varepsilon & 0 & 0 \\ 0 & \varepsilon & ig \\ 0 & -ig & \varepsilon \end{bmatrix}. \quad (1.52)$$

In the case of (1.52) the matrix of the system takes the form

$$\mathbf{A} = - \begin{bmatrix} \mathbf{K}_y \mathbf{E}^{-1} \mathbf{G} & \mathbf{0} & \mathbf{K}_y \mathbf{E}^{-1} \mathbf{K}_x & \mathbf{I} - \mathbf{K}_y \mathbf{E}^{-1} \mathbf{K}_y \\ \mathbf{K}_x \mathbf{E}^{-1} \mathbf{G} & \mathbf{0} & \mathbf{K}_x \mathbf{E}^{-1} \mathbf{K}_x - \mathbf{I} & -\mathbf{K}_x \mathbf{E}^{-1} \mathbf{K}_y \\ \mathbf{K}_y \mathbf{K}_x & \mathbf{E}^* - \mathbf{K}_y^2 & \mathbf{0} & \mathbf{0} \\ \mathbf{G} \mathbf{E}^{-1} \mathbf{G} + \mathbf{K}_x^2 - \mathbf{E} & -\mathbf{K}_x \mathbf{K}_y & \mathbf{G} \mathbf{E}^{-1} \mathbf{K}_x & -\mathbf{G} \mathbf{E}^{-1} \mathbf{K}_y \end{bmatrix}, \quad (1.53)$$

where $\mathbf{G} = \left[\left[\mathbf{g} \right] \right]$.

For the *equatorial geometry of magnetization* (the magnetization vector is parallel to the plane of layers and the direction of the axis Oy) $\theta_M = \varphi_M = \frac{\pi}{2}$. In this case from (1.49) we obtain:

$$\vec{\varepsilon} = \begin{bmatrix} \varepsilon & 0 & ig \\ 0 & \varepsilon & 0 \\ -ig & 0 & \varepsilon \end{bmatrix}. \quad (1.54)$$

For the tensor (1.54) the matrix of the system takes the form

$$\mathbf{A} = - \begin{bmatrix} \mathbf{0} & \mathbf{K}_y \mathbf{E}_2^{-1} \mathbf{H} \mathbf{E}^* & \mathbf{K}_y \mathbf{E}_2^{-1} \mathbf{K}_x & \mathbf{I} - \mathbf{K}_y \mathbf{E}_2^{-1} \mathbf{K}_y \\ \mathbf{0} & \mathbf{K}_x \mathbf{E}_2^{-1} \mathbf{H} \mathbf{E}^* & \mathbf{K}_x \mathbf{E}_2^{-1} \mathbf{K}_x - \mathbf{I} & -\mathbf{K}_x \mathbf{E}_2^{-1} \mathbf{K}_y \\ \mathbf{K}_y \mathbf{K}_x & \mathbf{E}^* - \mathbf{K}_y^2 - \mathbf{E}^* \mathbf{H} \mathbf{E}_2^{-1} \mathbf{H} \mathbf{E}^* & -\mathbf{E}^* \mathbf{H} \mathbf{E}_2^{-1} \mathbf{K}_x & \mathbf{E}^* \mathbf{H} \mathbf{E}_2^{-1} \mathbf{K}_y \\ \mathbf{K}_x^2 - \mathbf{E} & -\mathbf{K}_x \mathbf{K}_y & \mathbf{0} & \mathbf{0} \end{bmatrix} \quad (1.55)$$

1.1.2.4. Representation of the field inside the layer

For direct representation of the field in the layer, we consider the eigendecomposition of the matrix \mathbf{A} :

$$\mathbf{A} = \mathbf{W}\mathbf{\Lambda}\mathbf{W}^{-1}, \quad (1.56)$$

wherein $\mathbf{\Lambda} = \text{diag } \lambda_i$ is the diagonal matrix of eigenvalues of the matrix \mathbf{A} , and \mathbf{W} is the matrix of eigenvectors. Then the solution of system of differential equations (1.35) can be written as

$$\begin{bmatrix} \mathbf{S}_y \\ \mathbf{S}_x \\ \mathbf{U}_y \\ \mathbf{U}_x \end{bmatrix} = \mathbf{W} \exp(\mathbf{\Lambda} z') \mathbf{C}' = \mathbf{W} \exp(\mathbf{\Lambda} k_0 z) \mathbf{C}' = \sum_i c'_i \mathbf{w}_i \exp(\lambda_i k_0 z). \quad (1.57)$$

We split the last sum into two depending on the sign of the real part λ_i and write the expression in matrix notation:

$$\begin{aligned} \begin{bmatrix} \mathbf{S}_y \\ \mathbf{S}_x \\ \mathbf{U}_y \\ \mathbf{U}_x \end{bmatrix} &= \sum_i c'_i \mathbf{w}_i \exp(\lambda_i k_0 z) = \sum_{i: \text{Re}\lambda_i < 0} c_i \mathbf{w}_i \exp(\lambda_i k_0 (z - z_l)) + \\ &\quad \sum_{i: \text{Re}\lambda_i > 0} c_i \mathbf{w}_i \exp(\lambda_i k_0 (z - z_{l-1})) = \\ &= \mathbf{W}^{(-)} \exp(\mathbf{\Lambda}^{(-)} k_0 (z - z_l)) \mathbf{C}^{(-)} + \\ &\quad \mathbf{W}^{(+)} \exp(\mathbf{\Lambda}^{(+)} k_0 (z - z_{l-1})) \mathbf{C}^{(+)}, \end{aligned} \quad (1.58)$$

where $\mathbf{\Lambda}^{(+)}$ and $\mathbf{\Lambda}^{(-)}$ are the diagonal matrices of the eigenvalues whose the real parts are positive and negative, respectively, $\mathbf{W}^{(+)}$ and $\mathbf{W}^{(-)}$ are the corresponding eigenvector matrices, $\mathbf{C}^{(-)}$, $\mathbf{C}^{(+)}$ are the vectors of arbitrary constants. The representation (1.58) is suitable for numerical calculations. The exponent in (1.58) always has a negative real part. This ensures that there is no numerical overflow.

The procedure for calculating the eigenvectors and eigenvalues can in some cases be significantly speeded up taking into account the specific form of the matrix \mathbf{A} [4]. In particular, the matrix \mathbf{A} in (1.47), (1.48) and (1.51) has the following block structure:

$$\mathbf{A} = \begin{bmatrix} \mathbf{0} & \mathbf{A}_{12} \\ \mathbf{A}_{21} & \mathbf{0} \end{bmatrix}. \quad (1.59)$$

We write for \mathbf{A} the matrices of eigenvectors and eigenvalues in the form

$$\mathbf{W} = \begin{bmatrix} \mathbf{W}_{11} & \mathbf{W}_{12} \\ \mathbf{W}_{21} & \mathbf{W}_{22} \end{bmatrix}, \quad \mathbf{\Lambda} = \begin{bmatrix} \mathbf{\Lambda}_{11} & \mathbf{0} \\ \mathbf{0} & \mathbf{\Lambda}_{22} \end{bmatrix} \quad (1.60)$$

Since $\mathbf{A} = \mathbf{W}\mathbf{\Lambda}\mathbf{W}^{-1}$, then

$$\begin{aligned} \begin{bmatrix} \mathbf{0} & \mathbf{A}_{12} \\ \mathbf{A}_{21} & \mathbf{0} \end{bmatrix} \cdot \begin{bmatrix} \mathbf{W}_{11} & \mathbf{W}_{12} \\ \mathbf{W}_{21} & \mathbf{W}_{22} \end{bmatrix} &= \begin{bmatrix} \mathbf{W}_{11} & \mathbf{W}_{12} \\ \mathbf{W}_{21} & \mathbf{W}_{22} \end{bmatrix} \cdot \begin{bmatrix} \mathbf{\Lambda}_{11} & \mathbf{0} \\ \mathbf{0} & \mathbf{\Lambda}_{22} \end{bmatrix} \\ \begin{bmatrix} \mathbf{A}_{12}\mathbf{W}_{21} & \mathbf{A}_{12}\mathbf{W}_{22} \\ \mathbf{A}_{21}\mathbf{W}_{11} & \mathbf{A}_{21}\mathbf{W}_{12} \end{bmatrix} &= \begin{bmatrix} \mathbf{W}_{11}\mathbf{\Lambda}_{11} & \mathbf{W}_{12}\mathbf{\Lambda}_{22} \\ \mathbf{W}_{21}\mathbf{\Lambda}_{11} & \mathbf{W}_{22}\mathbf{\Lambda}_{22} \end{bmatrix} \end{aligned}$$

and we have:

$$\begin{aligned} \mathbf{A}_{12}\mathbf{A}_{21}\mathbf{W}_{11} &= \mathbf{A}_{12}\mathbf{W}_{21}\mathbf{\Lambda}_{11} = \mathbf{W}_{11}\mathbf{\Lambda}_{11}\mathbf{\Lambda}_{11}, \\ \mathbf{A}_{12}\mathbf{A}_{21}\mathbf{W}_{12} &= \mathbf{A}_{12}\mathbf{W}_{22}\mathbf{\Lambda}_{22} = \mathbf{W}_{12}\mathbf{\Lambda}_{22}\mathbf{\Lambda}_{22}. \end{aligned} \quad (1.61)$$

We introduce the matrix $\mathbf{B} = \mathbf{A}_{12}\mathbf{A}_{21}$ and write (1.61) in the form

$$\mathbf{B} \cdot \mathbf{W}_{11} = \mathbf{W}_{11}\mathbf{\Lambda}_{11}^2, \quad \mathbf{B} \cdot \mathbf{W}_{12} = \mathbf{W}_{12}\mathbf{\Lambda}_{22}^2. \quad (1.62)$$

According to (1.62) $\mathbf{W}_{11}, \mathbf{\Lambda}' = \mathbf{\Lambda}_{11}^2, \mathbf{W}_{12}, \mathbf{\Lambda}_{22}^2$ are the matrices of the eigenvectors and the diagonal matrices of the eigenvalues of the same matrix \mathbf{B} . Therefore

$$\mathbf{W}_{11} = \mathbf{W}_{12}, \quad \mathbf{\Lambda}_{22} = -\mathbf{\Lambda}_{11} \quad \text{and} \quad \mathbf{W}_{21} = \mathbf{A}_{21}\mathbf{W}_{11}\mathbf{\Lambda}_{11}^{-1}, \quad \mathbf{W}_{22} = -\mathbf{W}_{21}. \quad (1.63)$$

The relations (1.63) determine the eigenvalues and eigenvectors of the matrix \mathbf{A} by the eigenvalues and eigenvectors of the matrix \mathbf{B} half their size in the form:

$$\mathbf{W} = \begin{bmatrix} \mathbf{W}_{11} & \mathbf{W}_{11} \\ \mathbf{A}_{21}\mathbf{W}_{11}\sqrt{\mathbf{\Lambda}'}^{-1} & -\mathbf{A}_{21}\mathbf{W}_{11}\sqrt{\mathbf{\Lambda}'}^{-1} \end{bmatrix}, \quad \mathbf{\Lambda} = \begin{bmatrix} \sqrt{\mathbf{\Lambda}'} & \mathbf{0} \\ \mathbf{0} & -\sqrt{\mathbf{\Lambda}'} \end{bmatrix}. \quad (1.64)$$

In [4] it is pointed out that halving the dimensions of the eigenvalue problem is equivalent to transforming the system (1.35) of $4(2N+1)$ first-order differential equations to a system $2(2N+1)$ of second-order differential equations.

1.1.2.5. 'Stitching' of the electromagnetic field at the boundaries of layers

The general representation of the field in the layer was described above. To obtain a solution that satisfies the Maxwell's equations, it is necessary to equate the tangential components of the fields at the boundaries of the layers. Equating the tangential field components is equivalent to equating the functions (1.58) corresponding to the Fourier coefficients at each fixed z . We write preliminary solutions of (1.58) on the upper and lower boundaries of all the layers. For convenience, we assume that the matrix of eigenvectors \mathbf{W} is given by:

$$\mathbf{W} = [\mathbf{W}^{(-)} \quad \mathbf{W}^{(+)}]. \quad (1.65)$$

In addition, we introduce a vector of unknown constants \mathbf{C} as follows:

$$\mathbf{C} = \begin{bmatrix} \mathbf{C}^{(-)} \\ \mathbf{C}^{(+)} \end{bmatrix}. \quad (1.66)$$

In view of this notation the solution of (1.58) on the upper and lower boundaries of the layer has the form

$$\begin{bmatrix} \mathbf{S}_y(z_{l-1}) \\ \mathbf{S}_x(z_{l-1}) \\ \mathbf{U}_y(z_{l-1}) \\ \mathbf{U}_x(z_{l-1}) \end{bmatrix} = \mathbf{W}^{(-)} \mathbf{X}^{(-)} \mathbf{C}^{(-)} + \mathbf{W}^{(+)} \mathbf{C}^{(+)} = \mathbf{W} \begin{bmatrix} \mathbf{X}^{(-)} & \mathbf{0} \\ \mathbf{0} & \mathbf{I} \end{bmatrix} \mathbf{C} = \mathbf{N}\mathbf{C}, \quad (1.67)$$

$$\begin{bmatrix} \mathbf{S}_y(z_l) \\ \mathbf{S}_x(z_l) \\ \mathbf{U}_y(z_l) \\ \mathbf{U}_x(z_l) \end{bmatrix} = \mathbf{W}^{(-)} \mathbf{C}^{(-)} + \mathbf{W}^{(+)} \mathbf{X}^{(+)} \mathbf{C}^{(+)} = \mathbf{W} \begin{bmatrix} \mathbf{I} & \mathbf{0} \\ \mathbf{0} & \mathbf{X}^{(+)} \end{bmatrix} \mathbf{C} = \mathbf{M}\mathbf{C}, \quad (1.68)$$

where

$$\mathbf{X}^{(+)} = \exp(\mathbf{\Lambda}^{(+)} k_0 (z_l - z_{l-1})), \quad \mathbf{X}^{(-)} = \exp(-\mathbf{\Lambda}^{(-)} k_0 (z_l - z_{l-1})). \quad (1.69)$$

Equating the tangential components at the interface of the adjacent layers, we obtain the equations

$$\mathbf{M}_{l-1}\mathbf{C}_{l-1} = \mathbf{N}_l\mathbf{C}_l, \quad l = 2, \dots, L, \quad (1.70)$$

where the index $l = 2$ corresponds to the condition for the lower boundary of the upper layer, $l = L$ for the upper boundary of the lower layer.

The relations (1.70) must be supplemented by the conditions of the equality of the tangential components of the field above the structure of (1.20) and at the upper boundary of the 1st layer, as well as the field below the structure (1.21) and at the lower boundary of the L -th layer. Given that the components in the field in the region of the layers are represented by segments of the Fourier series with the dimension $2N + 1$, in representations of the field above and under the grating (1.20)–(1.22) we should also take $2N + 1$ waves at $-N \leq i \leq N$.

By adding these relations for the upper and lower boundaries of the diffractive structure, we obtain the following system of linear equations:

$$\begin{cases} \mathbf{D} + \mathbf{P}^{(U)} \mathbf{R} = \mathbf{N}_1 \mathbf{C}_1, \\ \mathbf{M}_{l-1} \mathbf{C}_{l-1} = \mathbf{N}_l \mathbf{C}_l, \quad l = 2, \dots, L, \\ \mathbf{M}_L \mathbf{C}_L = \mathbf{P}^{(D)} \mathbf{T}, \end{cases} \quad (1.71)$$

where \mathbf{R} and \mathbf{T} are the vectors of complex amplitudes of the reflected and transmitted orders, respectively. These vectors are of the form:

$$\mathbf{R} = \begin{bmatrix} \mathbf{R}_E \\ \mathbf{R}_H \end{bmatrix}, \quad \mathbf{T} = \begin{bmatrix} \mathbf{T}_E \\ \mathbf{T}_H \end{bmatrix}, \quad (1.72)$$

where \mathbf{R}_E and \mathbf{T}_E are the vectors of complex amplitudes of the E-waves, \mathbf{R}_H and \mathbf{T}_H are the vectors of complex amplitudes of the H-waves.

The vector \mathbf{D} in (1.71) represents the incident wave and has the form (see (1.13) for $\theta \rightarrow \pi - \theta$):

$$\mathbf{D} = \begin{bmatrix} \cos \theta \sin \varphi \cdot \boldsymbol{\delta}_i \\ \cos \theta \cos \varphi \cdot \boldsymbol{\delta}_i \\ -in_U \cos \varphi \cdot \boldsymbol{\delta}_i \\ in_U \sin \varphi \cdot \boldsymbol{\delta}_i \end{bmatrix} \cos \psi + \begin{bmatrix} \cos \varphi \cdot \boldsymbol{\delta}_i \\ -\sin \varphi \cdot \boldsymbol{\delta}_i \\ in_U \cos \theta \sin \varphi \cdot \boldsymbol{\delta}_i \\ in_U \cos \theta \cos \varphi \cdot \boldsymbol{\delta}_i \end{bmatrix} \sin \psi, \quad (1.73)$$

where δ_i is the column vector in which only one element, standing in the middle, is nonzero and is equal to one. Column vector δ_i has the dimension $2N + 1$ and vector \mathbf{D} the dimension $4(2N + 1)$.

The matrices $\mathbf{P}^{(U)}$ and $\mathbf{P}^{(D)}$ (1.71) correspond to the reflected and transmitted orders, respectively, and have the form

$$\mathbf{P}^{(p)} = \begin{bmatrix} -\cos \Theta^{(p)} \sin \Phi & \cos \Phi \\ -\cos \Theta^{(p)} \cos \Phi & -\sin \Phi \\ -in_p \cos \Phi & -in_p \cos \Theta^{(p)} \sin \Phi \\ in_p \sin \Phi & -in_p \cos \Theta^{(p)} \cos \Phi \end{bmatrix}, \quad p = U, D, \quad (1.74)$$

where Φ , $\Theta^{(p)}$ are the diagonal matrices of the angles determining the direction of the scattered diffraction orders. They satisfy the following relations:

$$\sin \Phi = \text{diag}_i \frac{k_y}{\sqrt{k_{x,i}^2 + k_y^2}}, \quad \cos \Phi = \text{diag}_i \frac{k_{x,i}}{\sqrt{k_{x,i}^2 + k_y^2}}, \quad (1.75)$$

$$\cos \Theta^{(U)} = \text{diag}_i \frac{k_{z,U,i}}{k_0 n_U}, \quad \cos \Theta^{(D)} = \text{diag}_i \frac{-k_{z,D,i}}{k_0 n_D}. \quad (1.76)$$

The expressions (1.73)–(1.74) follow directly from the general formulas (1.12) and (1.13) for a plane wave with the form of propagation constants of the orders (1.22) taken into account.

According to (1.71), the solution of the diffraction problem is reduced to solving a system of linear equations. The sequential expression of the coefficients \mathbf{C}_{l-1} in the layer with the index $(l-1)$ through the coefficients \mathbf{C}_l in the l -th layer allows to reduce the system (1.71) to a system of equations for the coefficients \mathbf{R} and \mathbf{T} . Indeed, from the last two equations in (1.71), we obtain

$$\mathbf{M}_{L-1} \mathbf{C}_{L-1} = \mathbf{N}_L \mathbf{M}_L^{-1} \mathbf{P}^{(D)} \mathbf{T}. \quad (1.77)$$

By substituting (1.77) into the equation with index $l = L-1$ in (1.71) we have

$$\mathbf{M}_{L-2} \mathbf{C}_{L-2} = \mathbf{N}_{L-1} \mathbf{M}_{L-1}^{-1} \mathbf{N}_L \mathbf{M}_L^{-1} \mathbf{P}^{(D)} \mathbf{T}. \quad (1.78)$$

Continuing this process to the equation with the index $l = 2$, we obtain

$$\mathbf{M}_1 \mathbf{C}_1 = \left(\prod_{l=2}^L \mathbf{N}_l \mathbf{M}_l^{-1} \right) \mathbf{P}^{(D)} \mathbf{T}. \quad (1.79)$$

Finally, substituting (1.79) in the first equation (1.71), we obtain the desired system of linear equations for the coefficients \mathbf{R} and \mathbf{T} in the form of:

$$\mathbf{D} + \mathbf{P}^{(U)} \mathbf{R} = \left(\prod_{l=1}^L \mathbf{N}_l \mathbf{M}_l^{-1} \right) \mathbf{P}^{(D)} \mathbf{T}. \quad (1.80)$$

Note that writing the system in this form allows to calculate the vectors \mathbf{R} and \mathbf{T} , but the calculation directly from (1.80) can lead to a numerical instability of the problem [3]. There are several numerically stable approaches [3, 18] to calculating the vectors \mathbf{R} and \mathbf{T} . We consider the so-called method of the scattering matrix [18].

1.1.2.6. The scattering matrix algorithm

Consider the Rayleigh expansion (1.20), (1.21) of the field above the structure, but instead of one incident wave (corresponding to the zeroth diffraction order), we consider a set of incident waves (respective orders $-N, \dots, N$). Then, the propagation constant can be described by the following expressions:

$$k_{x,m} = k_{x,0} + k_0 \cdot m \frac{\lambda}{d}, \quad m = -N, \dots, N; \quad (1.81)$$

$$k_{z,m}^R = \sqrt{k_0^2 \varepsilon_U - k_{x,m}^2}; \quad (1.82)$$

$$k_{z,m}^I = -\sqrt{k_0^2 \varepsilon_U - k_{x,m}^2}, \quad (1.83)$$

where $k_{z,m}^R$ are the propagation constants corresponding to the reflected orders; $k_{z,m}^I$ are the propagation constants of the waves incident on the structure from above.

Also, consider a set of waves incident on the structure from the substrate and write similar relations for the orders under the structure:

$$k_{z,m}^T = -\sqrt{k_0^2 \varepsilon_D - k_{x,m}^2}; \quad (1.84)$$

$$k_{z,m}^J = \sqrt{k_0^2 \varepsilon_D - k_{x,m}^2}, \quad (1.85)$$

where $k_{z,m}^T$ are the propagation constants corresponding to the transmitted orders; $k_{z,m}^J$ are the propagation constants of the waves incident on the structure from the substrate side.

In this case, when in addition to the $2N + 1$ reflected and $2N + 1$ transmitted diffraction orders there are also $2N + 1$ waves incident from above and $2N + 1$ waves incident from below, the calculation of complex amplitudes of diffraction orders consists in the determination of the \mathbf{S} -matrix satisfying the equation

$$\begin{bmatrix} \mathbf{T} \\ \mathbf{R} \end{bmatrix} = \mathbf{S} \begin{bmatrix} \mathbf{I}_1 \\ \mathbf{J}_{L+1} \end{bmatrix}, \quad (1.86)$$

where \mathbf{R} and \mathbf{T} are the vectors of the complex amplitudes of the reflected and transmitted diffraction orders, and \mathbf{I}_1 and \mathbf{J}_{L+1} are the vectors of the complex amplitudes of the waves incident on the structure from the top and the bottom, respectively. The matrix \mathbf{S} in (1.86) is called the *scattering matrix*. The scattering matrix \mathbf{S} is completely determined by the geometry of the structure, the optical properties of materials and the parameters of the incident radiation.

The difference between \mathbf{S} and the matrix of the system in the previously obtained expression (1.80) is that now it is necessary to consider not one incident wave but a set of waves incident on the structure from both the top and the substrate side. For the incident waves instead of (1.73) we will use the following expression at $p = U$:

$$\mathbf{D}^{(p)} = \begin{bmatrix} \cos \Theta^{(p)} \sin \Phi & \cos \Phi \\ \cos \Theta^{(p)} \cos \Phi & -\sin \Phi \\ -in_p \cos \Phi & in_p \cos \Theta^{(p)} \sin \Phi \\ in_p \sin \Phi & in_p \cos \Theta^{(p)} \cos \Phi \end{bmatrix}. \quad (1.87)$$

When $p = D$ the expression (1.87) describes the Fourier coefficients of the tangential components of the fields \mathbf{E} and \mathbf{H} corresponding to the waves incident on the structure from the ‘bottom’.

The system (1.71) will now take the form:

$$\begin{cases} \mathbf{D}^{(U)}\mathbf{I}_1 + \mathbf{P}^{(U)}\mathbf{R} = \mathbf{N}_1\mathbf{C}_1, \\ \mathbf{M}_{l-1}\mathbf{C}_{l-1} = \mathbf{N}_l\mathbf{C}_l, & l = 2, \dots, L, \\ \mathbf{M}_L\mathbf{C}_L = \mathbf{D}^{(D)}\mathbf{J}_{L+1} + \mathbf{P}^{(D)}\mathbf{T}, \end{cases} \quad (1.88)$$

We introduce the notation

$$\begin{aligned} \mathbf{I}_l &= \mathbf{X}_{l-1}^{(+)}\mathbf{C}_{l-1}^{(+)}; & \mathbf{J}_l &= \mathbf{X}_l^{(-)}\mathbf{C}_l^{(-)}; \\ \mathbf{R}_l &= \mathbf{C}_{l-1}^{(-)}; & \mathbf{T}_l &= \mathbf{C}_l^{(+)}, \end{aligned} \quad (1.89)$$

having the meaning of the complex amplitudes of the incident and scattered orders in each layer (see Fig. 1.2). Furthermore, to write system (1.88) in the most compact form, we introduce the notation

$$\begin{aligned} \mathbf{C}_0^{(-)} &= \mathbf{R}_1 = \mathbf{R}; & \mathbf{C}_{L+1}^{(+)} &= \mathbf{T}_{L+1} = \mathbf{T}; \\ \mathbf{X}_0^{(+)}\mathbf{C}_0^{(+)} &= \mathbf{I}_1; & \mathbf{X}_{L+1}^{(-)}\mathbf{C}_{L+1}^{(-)} &= \mathbf{J}_{L+1}; \\ \mathbf{W}_0^{(-)} &= \mathbf{P}^{(U)}; & \mathbf{W}_{L+1}^{(-)} &= \mathbf{D}^{(D)}; \\ \mathbf{W}_0^{(+)} &= \mathbf{D}^{(U)}; & \mathbf{W}_{L+1}^{(+)} &= \mathbf{P}^{(D)}. \end{aligned} \quad (1.90)$$

Then the system (1.88) can be written as

$$\left\{ \mathbf{W}_{l-1}^{(-)}\mathbf{R}_l + \mathbf{W}_{l-1}^{(+)}\mathbf{I}_l = \mathbf{W}_l^{(-)}\mathbf{J}_l + \mathbf{W}_l^{(+)}\mathbf{T}_l, \quad l = 1, \dots, L+1. \right. \quad (1.91)$$

$$\begin{array}{c} l-1 \\ \begin{array}{ccc} & \nearrow & \searrow \\ & \mathbf{R}_l & \mathbf{I}_l \\ & \nwarrow & \nearrow \end{array} \\ \frac{\Phi_1 = \mathbf{W}_{l-1}^{(-)}\overbrace{\mathbf{C}_{l-1}^{(-)}}^{\mathbf{R}_l} + \mathbf{W}_{l-1}^{(+)}\overbrace{\mathbf{X}_{l-1}^{(+)}\mathbf{C}_{l-1}^{(+)}}^{\mathbf{I}_l}}{\Phi_2 = \mathbf{W}_l^{(-)}\underbrace{\mathbf{X}_l^{(-)}\mathbf{C}_l^{(-)}}_{\mathbf{J}_l} + \mathbf{W}_l^{(+)}\underbrace{\mathbf{C}_l^{(+)}}_{\mathbf{T}_l}} \\ l \\ \begin{array}{ccc} & \nearrow & \searrow \\ & \mathbf{R}_{l+1} & \mathbf{I}_{l+1} \\ & \nwarrow & \nearrow \end{array} \\ \frac{\Phi_3 = \mathbf{W}_l^{(-)}\overbrace{\mathbf{C}_l^{(-)}}^{\mathbf{R}_{l+1}} + \mathbf{W}_l^{(+)}\overbrace{\mathbf{X}_l^{(+)}\mathbf{C}_l^{(+)}}^{\mathbf{I}_{l+1}}}{\Phi_4 = \mathbf{W}_{l+1}^{(-)}\underbrace{\mathbf{X}_{l+1}^{(-)}\mathbf{C}_{l+1}^{(-)}}_{\mathbf{J}_{l+1}} + \mathbf{W}_{l+1}^{(+)}\underbrace{\mathbf{C}_{l+1}^{(+)}}_{\mathbf{T}_{l+1}}} \\ l+1 \\ \begin{array}{ccc} & \nearrow & \searrow \\ & \mathbf{R}_{l+2} & \mathbf{I}_{l+2} \\ & \nwarrow & \nearrow \end{array} \end{array}$$

Fig. 1.2. Representation of fields at the bottom border of the $l-1$ -th layer (Φ_1), at the upper (Φ_2) and lower (Φ_3) borders of the l -th layer and the upper border of the $l+1$ -th layer (Φ_4).

We consider the numerically stable method for finding the scattering matrix of the multilayer structure [18]. We introduce the notation $\mathbf{S}^{(l)}$ for the scattering matrix, which connects the Fourier components of the field at the lower boundary of the structure and the lower boundary of the l -th layer

$$\begin{bmatrix} \mathbf{S}_{1,1}^{(l)} & \mathbf{S}_{1,2}^{(l)} \\ \mathbf{S}_{2,1}^{(l)} & \mathbf{S}_{2,2}^{(l)} \end{bmatrix} \begin{bmatrix} \mathbf{I}_{l+1} \\ \mathbf{J}_{l+1} \end{bmatrix} = \begin{bmatrix} \mathbf{T}_{l+1} \\ \mathbf{R}_{l+1} \end{bmatrix} \quad (1.92)$$

Also, we introduce the scattering matrix $\tilde{\mathbf{S}}^{(l)}$ linking the Fourier components of the field at the lower boundary of the structure and the upper boundary of l th layer:

$$\begin{bmatrix} \tilde{\mathbf{S}}_{1,1}^{(l)} & \tilde{\mathbf{S}}_{1,2}^{(l)} \\ \tilde{\mathbf{S}}_{2,1}^{(l)} & \tilde{\mathbf{S}}_{2,2}^{(l)} \end{bmatrix} \begin{bmatrix} \mathbf{T}_l \\ \mathbf{J}_{l+1} \end{bmatrix} = \begin{bmatrix} \mathbf{T}_{l+1} \\ \mathbf{J}_l \end{bmatrix}. \quad (1.93)$$

Consider the sequential method of constructing the scattering matrix structure, starting from the matrix $\tilde{\mathbf{S}}^{(L+1)} = \mathbf{I}$, where \mathbf{I} is the identity matrix. We consistently find the matrices $\mathbf{S}^{(l)}$ and $\tilde{\mathbf{S}}^{(l)}$ in the following sequence:

$$\mathbf{I} = \tilde{\mathbf{S}}^{(L+1)} \rightarrow \mathbf{S}^{(L)} \rightarrow \tilde{\mathbf{S}}^{(L)} \rightarrow \mathbf{S}^{(L-1)} \rightarrow \dots \rightarrow \tilde{\mathbf{S}}^{(1)} \rightarrow \mathbf{S}^{(0)} = \mathbf{S}. \quad (1.94)$$

Equalities (1.89) make it easy to find the matrix $\tilde{\mathbf{S}}^{(l)}$, knowing the matrix $\mathbf{S}^{(l)}$:

$$\tilde{\mathbf{S}}^{(l)} = \begin{bmatrix} \mathbf{I} & \mathbf{0} \\ \mathbf{0} & \mathbf{X}_l^{(-)} \end{bmatrix} \mathbf{S}^{(l)} \begin{bmatrix} \mathbf{X}_l^{(+)} & \mathbf{0} \\ \mathbf{0} & \mathbf{I} \end{bmatrix}. \quad (1.95)$$

We find the numerically stable equations for calculating the matrix $\mathbf{S}^{(l-1)}$ on the basis of the matrix $\tilde{\mathbf{S}}^{(l)}$. To do this, we write the equation of the system (1.91) with the number $l+1$ in the following matrix form:

$$\begin{bmatrix} \mathbf{W}_l^{(+)} & -\mathbf{W}_{l+1}^{(-)} \end{bmatrix} \begin{bmatrix} \mathbf{I}_{l+1} \\ \mathbf{J}_{l+1} \end{bmatrix} = \begin{bmatrix} \mathbf{W}_{l+1}^{(+)} & -\mathbf{W}_l^{(-)} \end{bmatrix} \begin{bmatrix} \mathbf{T}_{l+1} \\ \mathbf{R}_{l+1} \end{bmatrix} \quad (1.96)$$

We introduce the notation $\mathbf{H}^{(l)}$ by rewriting the expression (1.96) as follows:

$$\underbrace{\begin{bmatrix} \mathbf{W}_{l+1}^{(+)} & -\mathbf{W}_l^{(-)} \\ \mathbf{W}_l^{(+)} & -\mathbf{W}_{l+1}^{(-)} \end{bmatrix}^{-1}}_{\mathbf{H}^{(l)}} \begin{bmatrix} \mathbf{I}_{l+1} \\ \mathbf{J}_{l+1} \end{bmatrix} = \begin{bmatrix} \mathbf{T}_{l+1} \\ \mathbf{R}_{l+1} \end{bmatrix} \quad (1.97)$$

Matrix $\mathbf{H}^{(l)}$ has the meaning of the scattering matrix linking the field at the lower boundary of the l -th layer and the upper boundary of the $l+1$ -th layer. On the basis of expressions (1.92), (1.93), (1.97) it can be shown that the matrix $\mathbf{S}^{(l)}$ is calculated as

$$\mathbf{S}^{(l)} = \mathbf{H}^{(l)} \otimes \tilde{\mathbf{S}}^{(l+1)}, \quad (1.98)$$

where the associative operation “ \otimes ” is defined as follows [18]:

$$\begin{aligned} \begin{bmatrix} \mathbf{H}_{1,1} & \mathbf{H}_{1,2} \\ \mathbf{H}_{2,1} & \mathbf{H}_{2,2} \end{bmatrix} \otimes \begin{bmatrix} \mathbf{S}_{1,1} & \mathbf{S}_{1,2} \\ \mathbf{S}_{2,1} & \mathbf{S}_{2,2} \end{bmatrix} &= \\ &= \begin{bmatrix} \mathbf{S}_{1,1}(\mathbf{I} - \mathbf{H}_{1,2}\mathbf{S}_{2,1})^{-1}\mathbf{H}_{1,1} & \mathbf{S}_{1,2} + \mathbf{S}_{1,1}\mathbf{H}_{1,2}(\mathbf{I} - \mathbf{S}_{2,1}\mathbf{H}_{1,2})^{-1}\mathbf{S}_{2,2} \\ \mathbf{H}_{2,1} + \mathbf{H}_{2,2}\mathbf{S}_{2,1}(\mathbf{I} - \mathbf{H}_{1,2}\mathbf{S}_{2,1})^{-1}\mathbf{H}_{1,1} & \mathbf{H}_{2,2}(\mathbf{I} - \mathbf{S}_{2,1}\mathbf{H}_{1,2})^{-1}\mathbf{S}_{2,2} \end{bmatrix}. \end{aligned} \quad (1.99)$$

Note that in (1.95), (1.97), (1.99) there is no inversion of the ill-conditioned matrices, therefore, this method allows to find the scattering matrix of the structure \mathbf{S} and to avoid problems with numerical stability.

If a single plane wave of unit intensity is incident on the structure from above, complex transmission \mathbf{T} and reflection \mathbf{R} coefficients are found from (1.86):

$$\begin{bmatrix} \mathbf{T} \\ \mathbf{R} \end{bmatrix} = \mathbf{S} \begin{bmatrix} 1 \cdot \delta_i \\ 0 \cdot \delta_i \end{bmatrix}. \quad (1.100)$$

1.1.2.7. Calculation of the field distribution

In the calculation of the field distribution in the structure there may be the same problems with numerical stability as in the calculation of the complex amplitudes of diffraction orders. To construct the distribution of the field on the basis of expressions (1.27) and (1.58), it is necessary to know the values of the vectors $\mathbf{C}^{(-)}$, $\mathbf{C}^{(+)}$. Consider an iterative procedure for numerically-stable calculation of these vectors [19].

We assume that the vector \mathbf{R} of the complex amplitudes of the reflected orders and matrices $\mathbf{S}^{(l)}$, $\tilde{\mathbf{S}}^{(l)}$ is already calculated by the method described in the previous section.

We construct a recursive procedure for computing $\mathbf{C}_l^{(+)}$. From (1.97) at $l = 0$ we obtain the expression $\mathbf{C}_1^{(+)}$ in the form:

$$\mathbf{C}_1^{(+)} = \mathbf{T}_1 = \mathbf{H}_{1,1}^{(0)} \mathbf{I}_1 + \mathbf{H}_{1,2}^{(0)} \mathbf{J}_1 = \mathbf{H}_{1,1}^{(0)} \mathbf{I}_1 + \mathbf{H}_{1,2}^{(0)} \left(\mathbf{H}_{2,2}^{(0)} \right)^{-1} \left(\mathbf{R} - \mathbf{H}_{2,1}^{(0)} \mathbf{I}_1 \right). \quad (1.101)$$

Now, assuming that $\mathbf{C}_l^{(+)}$ is known we find expression $\mathbf{C}_{l+1}^{(+)} = \mathbf{T}_{l+1}$. From equation (1.93), taking into account $\mathbf{J}_{L+1} = 0$, we obtain

$$\mathbf{T}_{l+1} = \mathbf{C}_{l+1}^{(+)} = \left(\tilde{\mathbf{S}}_{1,1}^{(l+1)} \right)^{-1} \mathbf{T}_{L+1} = \left(\tilde{\mathbf{S}}_{1,1}^{(l+1)} \right)^{-1} \mathbf{T}. \quad (1.102)$$

We write the matrix $\mathbf{S}_{1,1}^{(l)}$ equation of (1.98) (1.99) in the form:

$$\mathbf{S}_{1,1}^{(l)} = \tilde{\mathbf{S}}_{1,1}^{(l+1)} \left(\mathbf{I} - \mathbf{H}_{1,2}^{(l)} \tilde{\mathbf{S}}_{2,1}^{(l+1)} \right)^{-1} \mathbf{H}_{1,1}^{(l)} \quad (1.103)$$

We express the matrix $\tilde{\mathbf{S}}_{1,1}^{(l)}$ from formula (1.95):

$$\tilde{\mathbf{S}}_{1,1}^{(l)} = \mathbf{S}_{1,1}^{(l)} \mathbf{X}_l^{(+)} . \quad (1.104)$$

We express from equations (1.103) the matrix $\left(\tilde{\mathbf{S}}_{1,1}^{(l+1)} \right)^{-1}$, and using the equation (1.104) we exclude matrix $\mathbf{S}_{1,1}^{(l)}$:

$$\left(\tilde{\mathbf{S}}_{1,1}^{(l+1)} \right)^{-1} = \left(\mathbf{I} - \mathbf{H}_{1,2}^{(l)} \tilde{\mathbf{S}}_{2,1}^{(l+1)} \right)^{-1} \mathbf{H}_{1,1}^{(l)} \left(\mathbf{S}_{1,1}^{(l)} \right)^{-1} = \left(\mathbf{I} - \mathbf{H}_{1,2}^{(l)} \tilde{\mathbf{S}}_{2,1}^{(l+1)} \right)^{-1} \mathbf{H}_{1,1}^{(l)} \mathbf{X}_l^{(+)} \left(\tilde{\mathbf{S}}_{1,1}^{(l)} \right)^{-1}. \quad (1.105)$$

Multiplying the left and right hand sides of (1.105) on the right by \mathbf{T} , with (1.102) taken into account, we finally obtain:

$$\mathbf{C}_{l+1}^{(+)} = \mathbf{T}_{l+1} = \left(\mathbf{I} - \mathbf{H}_{1,2}^{(l)} \tilde{\mathbf{S}}_{2,1}^{(l+1)} \right)^{-1} \mathbf{H}_{1,1}^{(l)} \mathbf{X}_l^{(+)} \mathbf{C}_l^{(+)} . \quad (1.106)$$

The recurrence relation (1.106) with the formula (1.101) allows to find $\mathbf{C}_l^{(+)}$ for all l . We now obtain a formula for finding $\mathbf{C}_l^{(-)} = \mathbf{R}_{l+1}$. From formula (1.92) at $\mathbf{J}_{L+1} = 0$ we have:

$$\mathbf{C}_l^{(-)} = \mathbf{R}_{l+1} = \mathbf{S}_{2,1}^{(l)} \mathbf{I}_{l+1} = \mathbf{S}_{2,1}^{(l)} \mathbf{X}_l^{(+)} \mathbf{C}_l^{(+)} . \quad (1.107)$$

1.1.2.8. Intensities of the diffraction orders

In the analysis of the field away from the grating researchers are usually not interested in complex amplitudes (1.72) and pay attention to the intensities of the reflected and transmitted propagating

diffraction orders. The propagating orders are determined by the real values $k_{z,p,m}$ in (1.22). The intensities of the diffraction orders are defined as the flux of the Umov–Poynting vector through the plane $z = \text{const}$, normalized to the corresponding flux of the incident wave [15]. Taking into account the expressions (1.16) and (1.17) the intensity of the orders can be found from the following expressions:

$$\mathbf{I}^R = \left| \frac{n_U \text{Re}(\cos \Theta^{(U)})}{n_U \cos \theta} \right| \left(|\mathbf{R}_E|^2 + |\mathbf{R}_H|^2 \right); \quad (1.108)$$

$$\mathbf{I}^T = \left| \frac{n_D \text{Re}(\cos \Theta^{(D)})}{n_U \cos \theta} \right| \left(|\mathbf{T}_E|^2 + |\mathbf{T}_H|^2 \right), \quad (1.109)$$

where the diagonal matrices $\cos \Theta^{(U)}$, $\cos \Theta^{(D)}$ are defined in (1.76), and squaring of vectors \mathbf{R}_E , \mathbf{R}_H , \mathbf{T}_E , \mathbf{T}_H is performed element wise. For evanescent diffraction orders $\text{Re}(\cos \Theta^{(p)}) = 0$, $p = U, D$, therefore their intensities are equal to zero.

In general, propagating diffraction orders are plane waves with elliptical polarization. Indeed, each diffraction order corresponds to the superposition of the E- and H-waves. Let E_E , E_H be the complex amplitude of the electric field at the E- and H-waves. Note that the electric field vectors in the E- and H-waves are perpendicular to each other and perpendicular to the direction of wave propagation. The addition of perpendicular oscillations results in the formation of an elliptically polarized wave. The polarization ellipse is characterized by two parameters: the angle ϕ of the major axis of the polarization ellipse and the ellipticity parameter χ [20]. The ellipticity parameter characterizes the ratio of the lengths of the a , b axes of the polarization ellipse in the form $\text{tg } \chi = a/b$. The parameters ϕ and χ are determined through complex amplitudes E_E , E_H as [20]

$$\begin{aligned} \text{tg}(2\phi) &= \frac{2 \text{Re}(E_E/E_H)}{1 - |E_E/E_H|^2}, \\ \sin(2\chi) &= \frac{2 \text{Im}(E_E/E_H)}{1 + |E_E/E_H|^2}. \end{aligned} \quad (1.110)$$

In conclusion, let us make a few remarks about the choice of the parameter N that determines the length of the segments of the Fourier series approximating the components of the electric and magnetic

fields in the grating. For a given N the number of calculated orders is equal to $2N + 1$, from $-N$ to $+N$. The parameter N must be greater than the number of propagating orders. If the grating consists only of dielectrics (all refractive indices are real numbers), and the parameter N satisfies this condition, the energy conservation law in the following form should be satisfied:

$$\sum I^R + \sum I^T = 1 \quad (1.111)$$

If the grating contains absorbing materials, the sum (1.111) should be less than one. In general, N is selected in computational experiment on the basis of the condition of stabilizing the intensities of the orders.

1.1.2.9. Numerical example

Consider the example of calculation of the intensities of diffraction orders of a binary grating. The grating geometry is shown in Fig. 1.3. The grating parameters are shown in the Fig. caption.

In the calculations the parameter N that determines the length of the segments of the Fourier series was $N = 20$. The calculations were carried out for the TM-polarized normally incident wave. The results of calculation of the reflection and transmission spectra of the grating (the intensities of diffraction orders) are shown in Fig. 1.4.

1.1.3. The Fourier modal method for three-dimensional periodic structures

Consider the described method in the case of three-dimensional periodic diffraction structures. The z -axis is perpendicular to the plane in which the diffraction grating is positioned. The functions of permittivity and magnetic permeability in the grating region are assumed to be periodic with respect to the variables x, y with periods d_x and d_y , respectively. As in the two-dimensional case, we assume

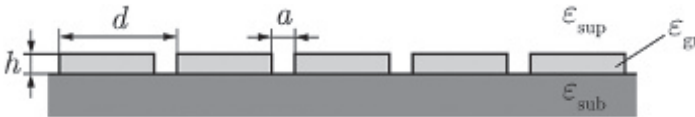


Fig. 1.3. The geometry of the binary grating (Parameters: $d = 1000$ nm, $a = 200$ nm, $h = 200$ nm, $\epsilon_{\text{sup}} = 1$, $\epsilon_{\text{gr}} = 4$, $\epsilon_{\text{sub}} = 2.25$).

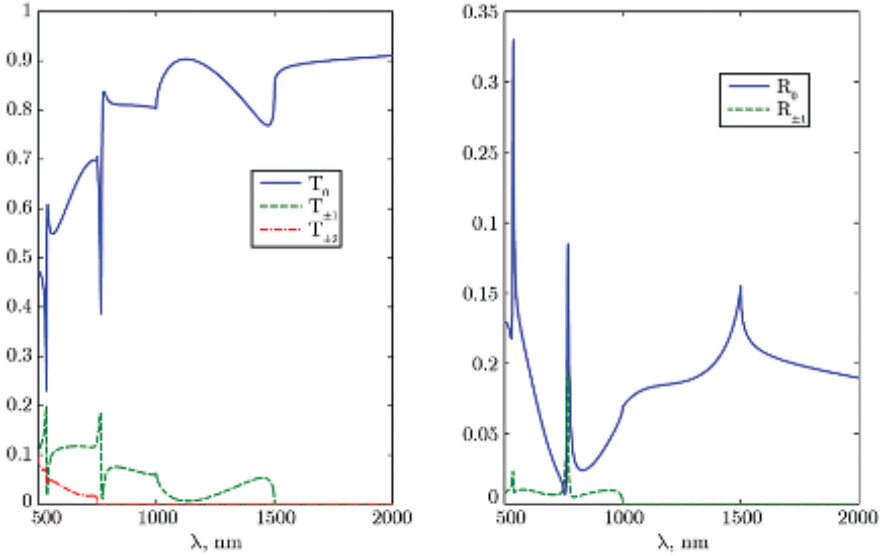


Fig. 1.4. The intensities of the reflected and transmitted diffraction orders.

that the diffraction grating is made up of L binary layers and the permittivity and permeability in each layer are independent of the variable z .

The method of solving the problem of diffraction in the three-dimensional case is similar to the two-dimensional case considered previously. The main details of the three-dimensional problem are given below.

Upon the plane wave diffraction on a three-dimensional diffraction grating, a set of reflected and transmitted diffraction orders is formed. In this case the field above and below the structure is as follows:

$$\Phi^U(x, y, z) = \Phi^{\text{inc}}(x, y, z) + \sum_n \sum_m \Phi_{n,m}^R(R_{n,m}) \exp(i(k_{x,n}x + k_{y,m}y + k_{z,U,n,m}z)), \quad (1.112)$$

$$\Phi^D(x, y, z) = \sum_n \sum_m \Phi_{n,m}^T(T_{n,m}) \exp(i(k_{x,n}x + k_{y,m}y - k_{z,D,n,m}(z - z_L))), \quad (1.113)$$

where $\Phi^{\text{inc}}(x, y, z)$ is the incident wave. The incident wave is assumed to be given in the form (1.19). The propagation constants of the diffraction orders with numbers (n, m) are described as follows:

$$\begin{aligned}
k_{x,n} &= k_0 \left(n_U \sin \theta \cos \varphi + n \frac{\lambda}{d_x} \right), \\
k_{y,m} &= k_0 \left(n_U \sin \theta \sin \varphi + m \frac{\lambda}{d_y} \right), \\
k_{z,p,n,m} &= \sqrt{\left(k_0 n_p \right)^2 - k_{x,n}^2 - k_{y,m}^2},
\end{aligned} \tag{1.114}$$

where as p , ‘U’ is taken for the reflected orders (the fields above the grating) and ‘D’ – for the transmitted ones (the field below the grating). The form of the propagation constants ensures that the two-dimensional quasi-periodicity condition is fulfilled:

$$\Phi^p(x + d_x, y + d_y, z) = \Phi^p(x, y, z) \exp\left(ik_{x,0} d_x + ik_{y,0} d_y \right), \quad p = \text{U, D}. \tag{1.115}$$

According to (1.115), the amplitude of the field does not change upon a shift along the x and y axes by integer multiples of the corresponding periods. The waves with the real $k_{z,p,n,m}$ are propagating, those with the imaginary value are evanescent.

The electromagnetic field in each layer, as in the two-dimensional case, is described by the basic Maxwell’s equations for the monochromatic field in the form (1.24)–(1.27). We represent the components of the electric and magnetic fields in the form of a two-dimensional Fourier series in the variables x, y :

$$\begin{cases}
E_x &= \sum_n \sum_m S_{x,n,m}(z) \exp\left(i(k_{x,n}x + k_{y,m}y) \right), \\
E_y &= \sum_n \sum_m S_{y,n,m}(z) \exp\left(i(k_{x,n}x + k_{y,m}y) \right), \\
E_z &= \sum_n \sum_m S_{z,n,m}(z) \exp\left(i(k_{x,n}x + k_{y,m}y) \right), \\
H_x &= -i \sum_n \sum_m U_{x,n,m}(z) \exp\left(i(k_{x,n}x + k_{y,m}y) \right), \\
H_y &= -i \sum_n \sum_m U_{y,n,m}(z) \exp\left(i(k_{x,n}x + k_{y,m}y) \right), \\
H_z &= -i \sum_n \sum_m U_{z,n,m}(z) \exp\left(i(k_{x,n}x + k_{y,m}y) \right).
\end{cases} \tag{1.116}$$

The equations (1.116) are written with the quasi-periodicity of the field components in the variables x, y taken into account. We restrict ourselves to a finite number of terms in the expansions

(1.116), corresponding to $-N_x \leq n \leq N_x$, $-N_y \leq m \leq N_y$. Substituting the expansion (1.116) into (1.26) and equating the coefficients of the same Fourier harmonics, we obtain a system of differential equations in the form

$$\left\{ \begin{array}{l} ik_0 \mathbf{K}_y \mathbf{S}_z - \frac{d\mathbf{S}_y}{dz} = k_0 (\mathbf{M}_{1,1} \mathbf{U}_x + \mathbf{M}_{1,2} \mathbf{U}_y + \mathbf{M}_{1,3} \mathbf{U}_z), \\ \frac{d\mathbf{S}_x}{dz} - ik_0 \mathbf{K}_x \mathbf{S}_z = k_0 (\mathbf{M}_{2,1} \mathbf{U}_x + \mathbf{M}_{2,2} \mathbf{U}_y + \mathbf{M}_{2,3} \mathbf{U}_z), \\ ik_0 \mathbf{K}_x \mathbf{S}_y - ik_0 \mathbf{K}_y \mathbf{S}_x = k_0 (\mathbf{M}_{3,1} \mathbf{U}_x + \mathbf{M}_{3,2} \mathbf{U}_y + \mathbf{M}_{3,3} \mathbf{U}_z), \\ ik_0 \mathbf{K}_y \mathbf{U}_z - \frac{d\mathbf{U}_y}{dz} = k_0 (\mathbf{E}_{1,1} \mathbf{S}_x + \mathbf{E}_{1,2} \mathbf{S}_y + \mathbf{E}_{1,3} \mathbf{S}_z), \\ \frac{d\mathbf{U}_x}{dz} - ik_0 \mathbf{K}_x \mathbf{U}_z = k_0 (\mathbf{E}_{2,1} \mathbf{S}_x + \mathbf{E}_{2,2} \mathbf{S}_y + \mathbf{E}_{2,3} \mathbf{S}_z), \\ ik_0 \mathbf{K}_x \mathbf{U}_y - ik_0 \mathbf{K}_y \mathbf{U}_x = k_0 (\mathbf{E}_{3,1} \mathbf{S}_x + \mathbf{E}_{3,2} \mathbf{S}_y + \mathbf{E}_{3,3} \mathbf{S}_z). \end{array} \right. \quad (1.117)$$

The form of the resulting system is the same as that of the system (1.31) for the two-dimensional case. The difference is in the details of the representation of vectors and matrices in the system. The vectors \mathbf{S}_x , \mathbf{S}_y , \mathbf{S}_z , \mathbf{U}_x , \mathbf{U}_y , \mathbf{U}_z in (1.117) are a row-wise one-dimensional representation of the matrices $S_{x,j,k}$, $S_{y,j,k}$, $S_{z,j,k}$, $U_{x,j,k}$, $U_{y,j,k}$, $U_{z,j,k}$, $-N_x \leq j \leq N_x$, $-N_y \leq k \leq N_y$. This means that the element of the vector \mathbf{S}_x with the number

$$l(i, j) = i(2N_y + 1) + j. \quad (1.118)$$

corresponds to the value $S_{x,l,j}$. The vectors introduced in this manner have the dimension $(2N_x + 1)(2N_y + 1)$ equal to the total number of the calculated diffraction orders. For example, the vector \mathbf{S}_x has the form

$$\mathbf{S}_x = \left[S_{x,-N_x,-N_y}, S_{x,-N_x,1-N_y}, \dots, S_{x,-N_x,N_y}, S_{x,1-N_x,-N_y}, S_{x,1-N_x,1-N_y}, \dots, S_{x,N_x,N_y} \right]^T \quad (1.119)$$

The matrices \mathbf{K}_x , \mathbf{K}_y , $\mathbf{E}_{i,j}$, $\mathbf{M}_{i,j}$ in (1.117) have the dimensions $(2N_x + 1)(2N_y + 1) \times (2N_x + 1)(2N_y + 1)$. The matrices \mathbf{K}_x and \mathbf{K}_y are defined by the following expressions:

$$\begin{aligned} K_{x,l(i,j),l(n,m)} &= k_{x,i} \delta_{i-n} \delta_{j-m} / k_0, \\ K_{y,l(i,j),l(n,m)} &= k_{y,j} \delta_{i-n} \delta_{j-m} / k_0, \end{aligned} \quad (1.120)$$

where $-N_x \leq i, n \leq N_x$, $-N_y \leq j, m \leq N_y$.

Consider the preliminary form of the matrices $\mathbf{E}_{i,j}$, $\mathbf{M}_{i,j}$ obtained by using the direct Laurent rules for the expansion of the product of the function into a Fourier series. The matrices $\mathbf{E}_{i,j}$, $\mathbf{M}_{i,j}$ consist of the Fourier coefficients of the permittivity and permeability tensors, the structure of the matrices is the same and has the form

$$T_{l(i,j),l(n,m)} = e_{i-n,j-m}, \quad (1.121)$$

where $e_{i,j}$ are the Fourier coefficients $-N_x \leq i, n \leq N_x$, $-N_y \leq j, m \leq N_y$.

Since the form of the systems of differential equations in the two-dimensional and three-dimensional cases is identical, all subsequent changes are also identical. The system of differential equations for the vectors \mathbf{S}_x , \mathbf{S}_y , \mathbf{U}_x , \mathbf{U}_y , in (1.117) also has the form (1.35)–(1.34). In particular, for a grating of an isotropic material $\varepsilon = \varepsilon(x,y)$ and $\mu = 1$ are the scalars, and the matrix of the differential equation system (1.35) has the form

$$\mathbf{A} = - \begin{bmatrix} \mathbf{0} & \mathbf{0} & \mathbf{K}_y \mathbf{E}^{-1} \mathbf{K}_x & \mathbf{I} - \mathbf{K}_y \mathbf{E}^{-1} \mathbf{K}_y \\ \mathbf{0} & \mathbf{0} & \mathbf{K}_x \mathbf{E}^{-1} \mathbf{K}_x - \mathbf{I} & -\mathbf{K}_x \mathbf{E}^{-1} \mathbf{K}_y \\ \mathbf{K}_y \mathbf{K}_x & \mathbf{E} - \mathbf{K}_y^2 & \mathbf{0} & \mathbf{0} \\ \mathbf{K}_x^2 - \mathbf{E} & -\mathbf{K}_x \mathbf{K}_y & \mathbf{0} & \mathbf{0} \end{bmatrix}, \quad (1.122)$$

where the matrix \mathbf{E} has the form (1.120) and is composed of the Fourier coefficients of functions $\varepsilon(x,y)$. The formula (1.122) is obtained from the general expressions (1.36) and (1.34) with

$$\begin{aligned} \mathbf{E}_{1,1} &= \mathbf{E}_{2,2} = \mathbf{E}_{3,3} = \mathbf{E}, \\ \mathbf{E}_{1,2} &= \mathbf{E}_{1,3} = \mathbf{E}_{2,1} = \mathbf{E}_{2,3} = \mathbf{E}_{3,1} = \mathbf{E}_{3,2} = \mathbf{0}, \\ \mathbf{M}_{1,1} &= \mathbf{M}_{2,2} = \mathbf{M}_{3,3} = \mathbf{I}, \\ \mathbf{M}_{1,2} &= \mathbf{M}_{1,3} = \mathbf{M}_{2,1} = \mathbf{M}_{2,3} = \mathbf{M}_{3,1} = \mathbf{M}_{3,2} = \mathbf{0}. \end{aligned} \quad (1.123)$$

Consider the transition to the spatial–frequency representation (1.117) using the correct rules of the Fourier expansion of the product of the functions. Derivation of the formulas is presented for the case of an isotropic material. In this case the system of Maxwell’s equations (1.26) contains only the following three products: εE_z , εE_x , εE_y .

The tangential component E_z is continuous, so the product εE_z is expanded into a Fourier series using the Laurent rules (1.40). In this case, the corresponding matrix $E_{3,3}$ (1.117) has the form (1.121).

We assume that the boundary between media with different dielectric constants in each layer is parallel to the axes [6]. Consider the product $D_x = \varepsilon E_x$. The product D_x is continuous at the sections of the boundaries between two media, parallel to the axis Oy . Indeed, in these areas $D_x = \varepsilon E_x$ is a normal component of the electric displacement. The component E_x and the function of the dielectric constant ε are discontinuous at these borders. Thus, the product $D_x = \varepsilon E_x$ is continuous with respect to x for any fixed y .

Accordingly, for the expansion of $D_x = \varepsilon E_x$ into the Fourier series in the variable x we use the inverse Laurent rule (1.41):

$$d_{x,i}(y,z) = \sum_n \varepsilon_{x i,n}(y) S_{x,n}(y,z), \quad (1.124)$$

where $d_{x,i}(y,z)$, $S_{x,n}(y,z)$ are the Fourier coefficients of the functions $D_x = \varepsilon E_x$, and $\varepsilon_{x i,n}(y)$ are the elements of the Toeplitz matrix $\llbracket 1/\varepsilon_x \rrbracket^{-1}$ formed from the Fourier coefficients with respect to the variable x of the function $1/\varepsilon(x,y)$. In the sections of the border between the media parallel to the axis Ox , component E_x is tangential and therefore continuous in the variable y . The Fourier coefficients $S_{x,n}(y,z)$ of the function E_x will also be continuous. Therefore, the expansion in (1.124) of the terms $\varepsilon_{x i,n}(y) S_{x,n}(y,z)$ into the Fourier series in the variable y is performed using the Laurent rule (1.40):

$$d_{x,i,j}(z) = \sum_{n,m} \varepsilon_{x i,n,j-m} S_{x,n,m}(z), \quad (1.125)$$

where $\varepsilon_{x i,n,j-m}$ is the Fourier coefficient with the number $(j-m)$ of the function $\varepsilon_{x i,n}(y)$.

Repeating similar reasoning for $D_y = \varepsilon E_y$, we obtain

$$d_{y,j}(x,z) = \sum_m \varepsilon_{y j,m}(x) S_{y,m}(x,z), \quad (1.126)$$

$$d_{y,i,j}(z) = \sum_{n,m} \varepsilon_{y i-n,j,m} S_{y,n,m}(z), \quad (1.127)$$

where $\varepsilon_{y j,m}(x)$ are the elements of the Toeplitz matrix $\llbracket 1/\varepsilon_y \rrbracket^{-1}$ formed from the Fourier coefficients in the variable y of the functions $1/\varepsilon(x,y)$, and $\varepsilon_{y i-n,j,m}$ is the Fourier coefficient with the number $(i-n)$ of the function $\varepsilon_{y j,m}$.

The equations (1.125) and (1.127) were obtained with the use of correct rules of expansion into a Fourier series of the products $D_x = \varepsilon E_x$, $D_y = \varepsilon E_y$. Accordingly, in transition from the system (1.26) to the spatial–frequency representation (1.117), the matrices $\mathbf{E}_{1,1}$, $\mathbf{E}_{2,2}$ will have the form

$$\begin{aligned} E_{1,1} l(i,n), l(j,m) &= \varepsilon_{x i,n,j-m}, \\ E_{2,2} l(i,n), l(j,m) &= \varepsilon_{y i-n,j,m} \end{aligned} \quad (1.128)$$

where $l(i,j)$ is defined in (1.118), $-N_x \leq i, n \leq N_x$, $-N_y \leq j, m \leq N_y$. The matrices (1.128) have the dimensions $(2N_x + 1)(2N_y + 1) \times (2N_x + 1)(2N_y + 1)$.

As a result, the matrix \mathbf{A} of the system of of the linear differential equations takes the form:

$$\mathbf{A} = - \begin{bmatrix} \mathbf{0} & \mathbf{0} & \mathbf{K}_y \mathbf{E}^{-1} \mathbf{K}_x & \mathbf{I} - \mathbf{K}_y \mathbf{E}^{-1} \mathbf{K}_y \\ \mathbf{0} & \mathbf{0} & \mathbf{K}_x \mathbf{E}^{-1} \mathbf{K}_x - \mathbf{I} & -\mathbf{K}_x \mathbf{E}^{-1} \mathbf{K}_y \\ \mathbf{K}_y \mathbf{K}_x & \mathbf{E}_{1,1} - \mathbf{K}_y^2 & \mathbf{0} & \mathbf{0} \\ \mathbf{K}_x^2 - \mathbf{E}_{2,2} & -\mathbf{K}_x \mathbf{K}_y & \mathbf{0} & \mathbf{0} \end{bmatrix}. \quad (1.129)$$

A detailed description of the correct rules of expansion into the Fourier series for the general case of the tensors of permittivity and permeability can be found in [8, 9].

Subsequent operations of the ‘stitching’ of the solutions at the layer boundaries and the numerically stable implementation of calculation of the matrix of the system of linear equations for the amplitudes of the diffraction orders are also the same. The matrices \mathbf{E}, \mathbf{F} in the systems of linear equations, representing the tangential field components (1.112), (1.113) at the upper and lower boundaries of the grating, also have the form of (1.74), where

$$\begin{aligned} \sin \Phi &= \text{diag}_{l(i,j)} \frac{k_{y,j}}{\sqrt{k_{x,i}^2 + k_{y,j}^2}}, \quad \cos \Phi = \text{diag}_{l(i,j)} \frac{k_{x,i}}{\sqrt{k_{x,i}^2 + k_{y,j}^2}}, \\ \cos \Phi^{(U)} &= \text{diag}_{l(i,j)} \frac{k_{z,U,i,j}}{k_0 n_U}, \quad \cos \Phi^{(D)} = \text{diag}_{l(i,j)} \frac{-k_{z,D,i,j}}{k_0 n_D}. \end{aligned} \quad (1.130)$$

Here $\text{diag}_{l(i,j)} f(i,j)$ denotes a diagonal matrix composed of elements $f(i,j)$ arranged in the ascending order of the magnitude of $l(i,j)$.

1.1.4. The Fourier modal method for two-dimensional non-periodic structures

1.1.4.1. The geometry of the structure and formulation of the problem

The Fourier modal method can be adapted to simulate the diffraction of the waveguide and plasmonic modes at inhomogeneities of the waveguide. Consider the method for the case when the geometry of the considered structure is independent of the coordinate y . In addition, we assume that, as before, the structure can be divided into regions and in each region $z_l < z < z_{l-1}$ the material parameters depend only on the coordinate x (Fig. 1.5). To apply the Fourier modal method we introduce the artificial periodization along the coordinate x , while for the elimination of the interaction between adjacent periods (i.e., to ensure vanishing of the electromagnetic field on the borders of the period) special absorbing layers are added to the boundaries of the period. These layers can be represented by multi-layered gradient absorbers or perfectly matched absorbing layers (PML) can be used [21, 22]. The gradient absorbing layers are layers in which the real part of the permittivity equals the permittivity of the adjacent medium, while the imaginary part, which characterizes absorption, increases while approaching the boundary of the period. A disadvantage of the gradient absorbing layers is non-zero reflection of incident radiation on them which increases substantially with increasing incidence angle. In some cases, this fact can substantially affect the solution of the problem with artificial periodization, decreasing the accuracy of the solution with respect to the solution of the original non-periodic problem. Reflections at the boundaries with absorbing layers are eliminated using perfectly matched absorbing layers described in the next section.

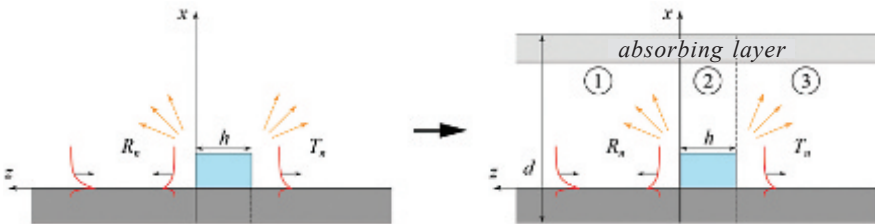


Fig. 1.5. The geometry of the problem of diffraction of surface plasmon polaritons in the aperiodic structure.

Unlike the standard version of the Fourier modal method, intended for the solution of the problem of diffraction on periodic structures, the result of the application of non-periodic modification will not be a set of intensities of diffraction orders but a set of the amplitudes of the reflected and transmitted modes.

1.1.4.2. Perfectly matched absorbing layers

Perfectly matched absorbing layers as anisotropic materials

Consider perfectly matched absorbing layers represented by a layer of anisotropic materials added to the boundaries of the period of the structure. The property of the perfectly matched absorbing layers to absorb incident radiation without back-reflection in this case is achieved by a special choice of the permittivity and permeability tensors.

To determine the type of tensor we consider initially an overview of the field of a plane electromagnetic waves in an anisotropic medium, described by the diagonal tensors of dielectric permittivity and magnetic permeability:

$$[\varepsilon] = \begin{pmatrix} \varepsilon_x & 0 & 0 \\ 0 & \varepsilon_y & 0 \\ 0 & 0 & \varepsilon_z \end{pmatrix}, \quad [\mu] = \begin{pmatrix} \mu_x & 0 & 0 \\ 0 & \mu_y & 0 \\ 0 & 0 & \mu_z \end{pmatrix}. \quad (1.131)$$

Since the properties of the medium do not depend on the variable z , the electric and magnetic fields have the form

$$\begin{aligned} \mathbf{E}(x, y, z) &= \mathbf{E}(x, y) \exp(ik_0 \gamma z), \\ \mathbf{H}(x, y, z) &= \mathbf{H}(x, y) \exp(ik_0 \gamma z). \end{aligned} \quad (1.132)$$

Substituting (1.131) into (1.3), we obtain:

$$\begin{aligned} \partial_y H_z - ik_0 \gamma H_y &= -ik_0 \varepsilon_x E_x, & \partial_y E_z - ik_0 \gamma E_y &= ik_0 \mu_x H_x, \\ -\partial_x H_z + ik_0 \gamma H_x &= -ik_0 \varepsilon_y E_y, & -\partial_x E_z + ik_0 \gamma E_x &= ik_0 \mu_y H_y, \\ \partial_x H_y - \partial_y H_x &= -ik_0 \varepsilon_z E_z, & \partial_x E_y - \partial_y E_x &= ik_0 \mu_z H_z, \end{aligned} \quad (1.133)$$

where $\partial_x f = \partial f / \partial x$. Using (1.133), we represent the tangential components by the components E_z, H_z in the form

$$\begin{aligned}
E_x &= \frac{-1}{ik_0(\varepsilon_x - \gamma^2 / \mu_y)} \left(\partial_y H_z + \frac{\gamma}{\mu_y} \cdot \partial_x E_z \right), \\
E_y &= \frac{1}{ik_0(\varepsilon_y - \gamma^2 / \mu_x)} \left(\partial_x H_z - \frac{\gamma}{\mu_x} \cdot \partial_y E_z \right), \\
H_x &= \frac{1}{ik_0(\mu_x - \gamma^2 / \varepsilon_y)} \left(\partial_y E_z - \frac{\gamma}{\varepsilon_y} \cdot \partial_x H_z \right), \\
H_y &= \frac{-1}{ik_0(\mu_y - \gamma^2 / \varepsilon_x)} \left(\partial_x E_z + \frac{\gamma}{\varepsilon_x} \cdot \partial_y H_z \right),
\end{aligned} \tag{1.134}$$

where E_z, H_z satisfy the equations

$$\begin{aligned}
&\frac{1}{(\mu_y - \gamma^2 / \varepsilon_x)} \left(\frac{\partial^2 E_z}{\partial x^2} + \frac{\gamma}{\varepsilon_x} \cdot \frac{\partial^2 H_z}{\partial x \partial y} \right) + \\
&+ \frac{1}{(\mu_x - \gamma^2 / \varepsilon_y)} \left(\frac{\partial^2 E_z}{\partial y^2} - \frac{\gamma}{\varepsilon_y} \cdot \frac{\partial^2 H_z}{\partial y \partial x} \right) = -k_0^2 \varepsilon_z E_z, \\
&\frac{1}{(\varepsilon_y - \gamma^2 / \mu_x)} \left(\frac{\partial^2 H_z}{\partial x^2} - \frac{\gamma}{\mu_x} \cdot \frac{\partial^2 E_z}{\partial x \partial y} \right) + \\
&+ \frac{1}{(\varepsilon_x - \gamma^2 / \mu_y)} \left(\frac{\partial^2 H_z}{\partial y^2} + \frac{\gamma}{\mu_y} \cdot \frac{\partial^2 E_z}{\partial y \partial x} \right) = -k_0^2 \mu_z H_z.
\end{aligned} \tag{1.135}$$

For an uniaxial anisotropic medium of the type

$$[\varepsilon] = \begin{pmatrix} \varepsilon & 0 & 0 \\ 0 & \varepsilon & 0 \\ 0 & 0 & \varepsilon_z \end{pmatrix}, \quad [\mu] = \begin{pmatrix} \mu & 0 & 0 \\ 0 & \mu & 0 \\ 0 & 0 & \mu_z \end{pmatrix} \tag{1.136}$$

we obtain from (1.135) that E_z, H_z satisfy the Helmholtz equation

$$\begin{aligned}
\frac{\partial^2 E_z}{\partial x^2} + \frac{\partial^2 E_z}{\partial y^2} &= -k_0^2 \varepsilon_z (\mu - \gamma^2 / \varepsilon) E_z, \\
\frac{\partial^2 H_z}{\partial x^2} + \frac{\partial^2 H_z}{\partial y^2} &= -k_0^2 \mu_z (\varepsilon - \gamma^2 / \mu) H_z.
\end{aligned} \tag{1.137}$$

Solving (1.137) by separation of variables, we obtain

$$\begin{aligned} E_z(x, y, z) &= \exp\left(ik_0\sqrt{\varepsilon_z\mu}(\alpha x + \beta y) \pm ik_0\gamma z\right), \\ H_z(x, y, z) &= \exp\left(ik_0\sqrt{\varepsilon_z\mu}(\alpha x + \beta y) \pm ik_0\gamma_1 z\right), \end{aligned} \quad (1.138)$$

where

$$\gamma = \sqrt{\varepsilon\mu}\sqrt{1 - \alpha^2 - \beta^2}, \quad \gamma_1 = \mu\sqrt{\varepsilon/\mu - (\alpha^2 + \beta^2)\varepsilon_z/\mu_z}. \quad (1.139)$$

Next, we consider the E- and H-type waves. For the E-wave $E_z \neq 0, H_z = 0$, and for the H-wave $H_z \neq 0, E_z = 0$. From (1.134) (1.138) for the E-waves we get

$$\begin{aligned} E_x &= \frac{\mp\gamma}{ik_0(\varepsilon\mu - \gamma^2)} \cdot \partial_x E_z = \frac{\mp\alpha\gamma\sqrt{\varepsilon_z\mu}}{(\mu\varepsilon - \gamma^2)} \cdot \exp\left(ik_0\sqrt{\varepsilon_z\mu}(\alpha x + \beta y) \pm ik_0\gamma z\right), \\ E_y &= \frac{\mp\gamma}{ik_0(\varepsilon\mu - \gamma^2)} \cdot \partial_y E_z = \frac{\mp\gamma\beta\sqrt{\varepsilon_z\mu}}{(\varepsilon\mu - \gamma^2)} \cdot \exp\left(ik_0\sqrt{\varepsilon_z\mu}(\alpha x + \beta y) \pm ik_0\gamma z\right), \\ H_x &= \frac{\varepsilon}{ik_0(\mu\varepsilon - \gamma^2)} \partial_y E_z = \frac{\varepsilon\beta\sqrt{\varepsilon_z\mu}}{(\mu\varepsilon - \gamma^2)} \cdot \exp\left(ik_0\sqrt{\varepsilon_z\mu}(\alpha x + \beta y) \pm ik_0\gamma z\right), \\ H_y &= \frac{-\varepsilon}{ik_0(\mu\varepsilon - \gamma^2)} \partial_x E_z = \frac{-\varepsilon\alpha\sqrt{\varepsilon_z\mu}}{(\mu\varepsilon - \gamma^2)} \cdot \exp\left(ik_0\sqrt{\varepsilon_z\mu}(\alpha x + \beta y) \pm ik_0\gamma z\right). \end{aligned} \quad (1.140)$$

Since the solution of the diffraction problem requires the imposition of conditions of equality of the tangential components of the fields at the interface, it is convenient to introduce the following four-component vector of the tangential components:

$$\mathbf{E}_E = \begin{pmatrix} E_x \\ H_y \\ E_y \\ H_x \end{pmatrix} = \frac{1}{\sqrt{\gamma\varepsilon(\alpha^2 + \beta^2)}} \begin{pmatrix} \mp\alpha\gamma \\ -\varepsilon\alpha \\ \mp\gamma\beta \\ \varepsilon\beta \end{pmatrix} \exp\left(ik_0\sqrt{\varepsilon_z\mu}(\alpha x + \beta y) \pm ik_0\gamma z\right) \quad (1.141)$$

Vector (1.141) is written with a normalizing factor chosen from the condition that the unit z -component of the Poynting vector $S_z = |E_x H_y - E_y H_x|$ is unity.

From (1.134) and (1.138) for the H-wave we get

$$\begin{aligned}
 E_x &= \frac{-\mu}{ik_0(\varepsilon\mu - \gamma_1^2)} \partial_y H_z = \frac{-\mu\beta\sqrt{\varepsilon_z\mu}}{(\varepsilon\mu - \gamma_1^2)} \cdot \exp\left(ik_0\sqrt{\varepsilon_z\mu}(\alpha x + \beta y) \pm ik_0\gamma_1 z\right), \\
 H_y &= \frac{\mp\gamma_1}{ik_0(\mu - \gamma_1^2)} \cdot \partial_y H_z = \frac{\mp\gamma_1\beta\sqrt{\varepsilon_z\mu}}{(\mu - \gamma_1^2)} \cdot \exp\left(ik_0\sqrt{\varepsilon_z\mu}(\alpha x + \beta y) \pm ik_0\gamma_1 z\right), \\
 E_y &= \frac{\mu}{ik_0(\varepsilon\mu - \gamma_1^2)} \cdot \partial_x H_z = \frac{\mu\alpha\sqrt{\varepsilon_z\mu}}{(\varepsilon\mu - \gamma_1^2)} \cdot \exp\left(ik_0\sqrt{\varepsilon_z\mu}(\alpha x + \beta y) \pm ik_0\gamma_1 z\right), \\
 H_x &= \frac{\mp\gamma_1}{ik_0(\mu\varepsilon - \gamma_1^2)} \cdot \partial_x H_z = \frac{\mp\gamma_1\alpha\sqrt{\varepsilon_z\mu}}{(\mu\varepsilon - \gamma_1^2)} \cdot \exp\left(ik_0\sqrt{\varepsilon_z\mu}(\alpha x + \beta y) \pm ik_0\gamma_1 z\right).
 \end{aligned} \tag{1.142}$$

Similarly to (1.141), we introduce the vector of the tangential components of the H-wave in the form

$$\mathbf{E}_H = \begin{pmatrix} E_x \\ H_y \\ E_y \\ H_x \end{pmatrix} = \frac{1}{\sqrt{\gamma_1\mu(\alpha^2 + \beta^2)}} \begin{pmatrix} -\mu\beta \\ \mp\gamma_1\beta \\ \mu\alpha \\ \mp\gamma_1\alpha \end{pmatrix} \exp\left(ik_0\sqrt{\varepsilon_z\mu}(\alpha x + \beta y) \pm ik_0\gamma_1 z\right). \tag{1.143}$$

Fresnel equations. We write the Fresnel equations for the interface between a homogeneous dielectric and a medium described by the tensor (1.136). Without the loss of generality, we assume that the interface is the plane $z = 0$. We also assume that in the region $z > 0$ there is a homogeneous dielectric, and at $z < 0$ – the anisotropic medium (1.136).

Suppose that a plane wave impinges on the interface from the side of the homogeneous dielectric. The plane wave is represented as a superposition of the E- and H-waves. In a general case, upon the reflection and refraction of the incident wave at the interface reflected and refracted waves will be formed as a superposition of the E- and H-waves.

Assuming in (1.141) and (1.143) $\varepsilon = \varepsilon_z = \varepsilon_0$, $\mu = \mu_z = \mu_0$, we write the E- and H-waves incident and reflected from the interface

$$\mathbf{E}_{inc,E} = \frac{1}{\sqrt{\gamma_0 \varepsilon_0 (\alpha_0^2 + \beta_0^2)}} \begin{pmatrix} \alpha_0 \gamma_0 \\ -\varepsilon_0 \alpha_0 \\ \gamma_0 \beta_0 \\ \varepsilon_0 \beta_0 \end{pmatrix} \exp\left(ik_0 \sqrt{\varepsilon_0 \mu_0} (\alpha_0 x + \beta_0 y) - ik_0 \gamma_0 z\right),$$

$$\mathbf{E}_{inc,H} = \frac{1}{\sqrt{\gamma_0 \mu_0 (\alpha_0^2 + \beta_0^2)}} \begin{pmatrix} -\mu_0 \beta_0 \\ \gamma_0 \beta_0 \\ \mu_0 \alpha_0 \\ \gamma_0 \alpha_0 \end{pmatrix} \exp\left(ik_0 \sqrt{\varepsilon_0 \mu_0} (\alpha_0 x + \beta_0 y) - ik_0 \gamma_0 z\right),$$
(1.144)

$$\mathbf{E}_{ref,E} = \frac{1}{\sqrt{\gamma_0 \varepsilon_0 (\alpha_0^2 + \beta_0^2)}} \begin{pmatrix} -\alpha_0 \gamma_0 \\ -\varepsilon_0 \alpha_0 \\ -\gamma_0 \beta_0 \\ \varepsilon_0 \beta_0 \end{pmatrix} \exp\left(ik_0 \sqrt{\varepsilon_0 \mu_0} (\alpha_0 x + \beta_0 y) + ik_0 \gamma_0 z\right),$$

$$\mathbf{E}_{ref,H} = \frac{1}{\sqrt{\gamma_0 \mu_0 (\alpha_0^2 + \beta_0^2)}} \begin{pmatrix} -\mu_0 \beta_0 \\ -\gamma_0 \beta_0 \\ \mu_0 \alpha_0 \\ -\gamma_0 \alpha_0 \end{pmatrix} \exp\left(ik_0 \sqrt{\varepsilon_0 \mu_0} (\alpha_0 x + \beta_0 y) + ik_0 \gamma_0 z\right),$$
(1.145)

where $\gamma_0 = \sqrt{\varepsilon_0 \mu_0} \sqrt{1 - \alpha_0^2 - \beta_0^2}$. ‘inc’ and ‘ref’ in the subscripts of the waves in (1.144) and (1.145) denote the incident and reflected waves, respectively.

If $z > 0$ the field is a superposition of the incident and reflected waves

$$\mathbf{E}_{z>0}(\mathbf{x}) = I_E \mathbf{E}_{inc,E}(\mathbf{x}) + I_H \mathbf{E}_{inc,H}(\mathbf{x}) + R_E \mathbf{E}_{ref,E}(\mathbf{x}) + R_H \mathbf{E}_{ref,H}(\mathbf{x}),$$
(1.146)

where $\mathbf{x} = (x, y, z)$, I_E , I_H are the coefficients of the E- and H-waves for the incident wave, and R_E , R_H are the reflection coefficients. The transmitted field $z < 0$ has the form:

$$\mathbf{E}_{z<0}(\mathbf{x}) = T_E \cdot \mathbf{E}_{tr,E}(\mathbf{x}) + T_H \cdot \mathbf{E}_{tr,H}(\mathbf{x}),$$
(1.147)

where T_E , T_H are the transmission coefficients,

$$\mathbf{E}_{r,E} = \frac{1}{\sqrt{\gamma\varepsilon(\alpha^2 + \beta^2)}} \begin{pmatrix} \alpha\gamma \\ -\varepsilon\alpha \\ \gamma\beta \\ \varepsilon\beta \end{pmatrix} \exp\left(ik_0\sqrt{\varepsilon_z\mu}(\alpha x + \beta y) - ik_0\gamma z\right),$$

$$\mathbf{E}_{r,H} = \frac{1}{\sqrt{\gamma_1\mu(\alpha^2 + \beta^2)}} \begin{pmatrix} -\mu\beta \\ \gamma_1\beta \\ \mu\alpha \\ \gamma_1\alpha \end{pmatrix} \exp\left(ik_0\sqrt{\varepsilon_z\mu}(\alpha x + \beta y) - ik_0\gamma_1 z\right),$$

(1.148)

where $\gamma = \sqrt{\varepsilon\mu}\sqrt{1 - \alpha^2 - \beta^2}$, $\gamma_1 = \mu\sqrt{\varepsilon/\mu - (\alpha^2 + \beta^2)}\varepsilon_z/\mu_z$.

To determine the reflection and transmission coefficients, we write the condition of equality of the tangential components at $z = 0$ ($\mu_0 = 1$):

$$\frac{I_E}{\sqrt{\gamma_0\varepsilon_0(\alpha_0^2 + \beta_0^2)}} \begin{pmatrix} \gamma_0\alpha_0 \\ -\varepsilon_0\alpha_0 \\ \gamma_0\beta_0 \\ \varepsilon_0\beta_0 \end{pmatrix} + \frac{I_H}{\sqrt{\gamma_0(\alpha_0^2 + \beta_0^2)}} \begin{pmatrix} -\beta_0 \\ \gamma_0\beta_0 \\ \alpha_0 \\ \gamma_0\alpha_0 \end{pmatrix} + \frac{R_E}{\sqrt{\gamma_0\varepsilon_0(\alpha_0^2 + \beta_0^2)}} \begin{pmatrix} -\gamma_0\alpha_0 \\ -\varepsilon_0\alpha_0 \\ -\gamma_0\beta_0 \\ \varepsilon_0\beta_0 \end{pmatrix} +$$

$$+ \frac{R_H}{\sqrt{\gamma_0(\alpha_0^2 + \beta_0^2)}} \begin{pmatrix} -\beta_0 \\ -\gamma_0\beta_0 \\ \alpha_0 \\ -\gamma_0\alpha_0 \end{pmatrix} = \frac{T_E}{\sqrt{\gamma\varepsilon(\alpha^2 + \beta^2)}} \begin{pmatrix} \alpha\gamma \\ -\varepsilon\alpha \\ \gamma\beta \\ \varepsilon\beta \end{pmatrix} + \frac{T_H}{\sqrt{\gamma_1\mu(\alpha^2 + \beta^2)}} \begin{pmatrix} -\mu\beta \\ \gamma_1\beta \\ \mu\alpha \\ \gamma_1\alpha \end{pmatrix}.$$

(1.149)

The refraction law should be satisfied in this case;

$$\alpha_0\sqrt{\varepsilon_0} = \alpha\sqrt{\varepsilon_z\mu}, \quad \beta_0\sqrt{\varepsilon_0} = \beta\sqrt{\varepsilon_z\mu}$$

(1.150)

In the particular case

$$[\varepsilon] = \varepsilon_0 \begin{pmatrix} a & 0 & 0 \\ 0 & a & 0 \\ 0 & 0 & 1/a \end{pmatrix}, \quad [\mu] = \begin{pmatrix} a & 0 & 0 \\ 0 & a & 0 \\ 0 & 0 & 1/a \end{pmatrix}$$

(1.151)

we obtain

$$\alpha = \alpha_0, \beta = \beta_0, \gamma = \gamma_1 = a\sqrt{\varepsilon_0}\sqrt{1 - \alpha_0^2 - \beta_0^2} = a\gamma_0. \quad (1.152)$$

In this case, the equation (1.149) takes the form

$$\begin{aligned} & \frac{I_E}{\sqrt{\gamma_0\varepsilon_0(\alpha_0^2 + \beta_0^2)}} \begin{pmatrix} \gamma_0\alpha_0 \\ -\varepsilon_0\alpha_0 \\ \gamma_0\beta_0 \\ \varepsilon_0\beta_0 \end{pmatrix} + \frac{I_H}{\sqrt{\gamma_0(\alpha_0^2 + \beta_0^2)}} \begin{pmatrix} -\beta_0 \\ \gamma_0\beta_0 \\ \alpha_0 \\ \gamma_0\alpha_0 \end{pmatrix} + \frac{R_E}{\sqrt{\gamma_0\varepsilon_0(\alpha_0^2 + \beta_0^2)}} \begin{pmatrix} -\gamma_0\alpha_0 \\ -\varepsilon_0\alpha_0 \\ -\gamma_0\beta_0 \\ \varepsilon_0\beta_0 \end{pmatrix} + \\ & + \frac{R_H}{\sqrt{\gamma_0(\alpha_0^2 + \beta_0^2)}} \begin{pmatrix} -\beta_0 \\ -\gamma_0\beta_0 \\ \alpha_0 \\ -\gamma_0\alpha_0 \end{pmatrix} = \frac{T_E}{\sqrt{\gamma_0\varepsilon_0(\alpha_0^2 + \beta_0^2)}} \begin{pmatrix} \alpha_0\gamma_0 \\ -\varepsilon_0\alpha_0 \\ \gamma_0\beta_0 \\ \varepsilon_0\beta_0 \end{pmatrix} + \frac{T_H}{\sqrt{\gamma_0(\alpha_0^2 + \beta_0^2)}} \begin{pmatrix} -\beta_0 \\ \gamma_0\beta_0 \\ \alpha_0 \\ \gamma_0\alpha_0 \end{pmatrix}. \end{aligned} \quad (1.153)$$

It is easy to see that the solution of (1.153) is as follows:

$$R_E = R_H = 0, \quad T_H = I_H, \quad T_E = I_E. \quad (1.154)$$

According to (1.154), medium (1.151) does not reflect the incident waves. At complex $a = a' + ia''$ in (1.151) the transmitted waves (1.148) will be evanescent. The rate of decay is determined by the imaginary part a'' . Thus, a layer of material (1.151) at complex a is a perfectly matched absorbing layer.

When $\beta_0 = 0$ in (1.144) the direction vector of the incident wave lies in the plane xOz . In the case of ‘planar incidence’ the E-wave corresponds to a wave with TM-polarization and the H-wave to a wave with TE-polarization.

For the incident wave with TM-polarization the medium (1.151) takes the form

$$[\varepsilon] = \varepsilon_0 \begin{pmatrix} a & 0 & 0 \\ 0 & a & 0 \\ 0 & 0 & 1/a \end{pmatrix}, \quad \mu = a. \quad (1.155)$$

Indeed, it is easy to show that under the condition (1.155), $\beta_0 = 0$ and $I_H = 0$ the solution of (1.149) has the form

$$R_E = R_H = 0, \quad T_H = 0, \quad T_E = I_E. \quad (1.156)$$

According to (1.156), the medium (1.155) does not reflect the incident waves.

Similarly, for the incident wave with TE-polarization the following condition is sufficient

$$\varepsilon = \varepsilon_0 a, \quad [\mu] = \begin{pmatrix} a & 0 & 0 \\ 0 & a & 0 \\ 0 & 0 & 1/a \end{pmatrix}. \quad (1.157)$$

In the case of (1.157) the solution of (1.149) with $\beta_0 = 0$ and $I_H = 0$ has the form

$$R_E = R_H = 0, \quad T_H = I_H, \quad T_E = 0. \quad (1.158)$$

Perfectly matched absorbing layers as a complex coordinate transformation

We now introduce the perfectly matched absorbing layers as a complex coordinate transformation [23]. For simplicity, consider the case of diffraction of a TM-polarized wave (in particular, the plasmonic modes – the geometry of the structure is shown on the left in Fig. 1.6) on the structure composed of isotropic materials. In this case, the electric and magnetic fields have the form $\mathbf{E} = (E_x, 0, E_z)$, $\mathbf{H} = (0, H_y, 0)$. In each of the layers of the structure at $\mu = 1$ we can obtain the Helmholtz equation for the component H_y from Maxwell's equations (1.24):

$$\frac{\partial^2 H_y}{\partial z^2} + \varepsilon(x) \frac{\partial}{\partial x} \left[\frac{1}{\varepsilon(x)} \frac{\partial H_y}{\partial x} \right] + k_0^2 \varepsilon(x) H_y = 0. \quad (1.159)$$

Equation (1.159) is written in a general form and is valid for both the initial non-periodic problem and, for example, for the problem of diffraction of the TM-polarized wave on a diffraction structure with one-dimensional periodicity. Note that in solving the diffraction problem by the Fourier modal method, equation (1.159), which describes the field in the layer of the structure, is reduced to a second system of differential equations in (1.48).

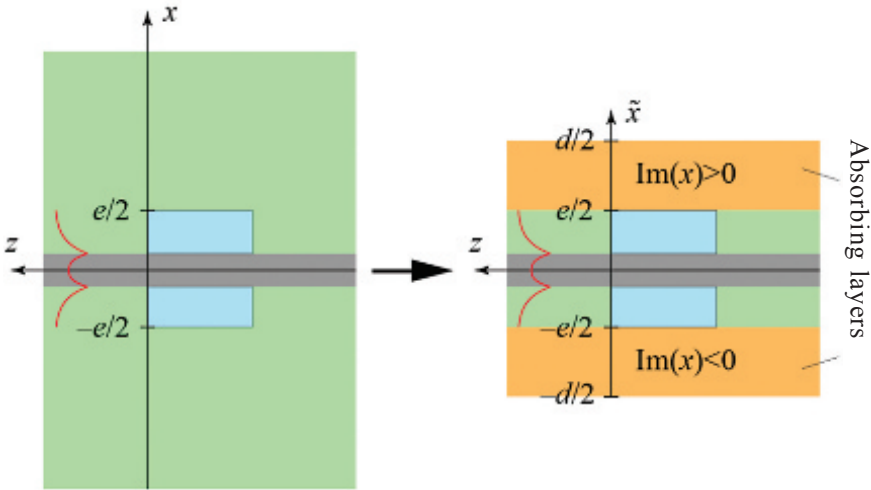


Fig. 1.6. The transition to a non-periodic task using perfectly matched absorbing layers in the form of coordinate transformations.

Suppose we are interested in the solution of the original aperiodic problem in the region $|x| > e/2$ in addition, the regions $|x| > e/2$ are homogeneous (Fig. 1.6). Note that because of physical reasons (absence of incident waves apart from the incident waveguide or plasmonic mode) the regions $|x| > e/2$ contain only the waves propagating from the structure (in the direction of increase $|x| > e/2$).

As indicated above, to solve a non-periodic problem by the Fourier modal method it is necessary to introduce artificial periodization with a certain period $d > e$ so as to eliminate the interaction between adjacent periods. To do this, it is necessary to ensure that the components of the electromagnetic field at the boundaries between periods are equal to zero. Consider the analytic continuation of the solution of equation (1.159) for the original problem in the variable x in the complex plane: $x = x' + ix''$. Note that the propagating waves are evanescent in this case. Indeed, for waves propagating in the positive direction of the x axis ($k_x > 0$), we get:

$$\exp(ik_x x) = \exp(ik_x x') \exp(-k_x x''). \quad (1.160)$$

Thus, these waves become evanescent when $x'' \rightarrow +\infty$. Similarly, the waves propagating in the negative direction of the axis x , decay when $x'' \rightarrow -\infty$. Thus, we consider the solution of (1.159) on the contour in the complex plane having the form shown in Fig. 1.7.

The horizontal dashed line shows the real axis, the vertical dotted lines – the area $x'/d \in [-e/(2d), e/(2d)]$.

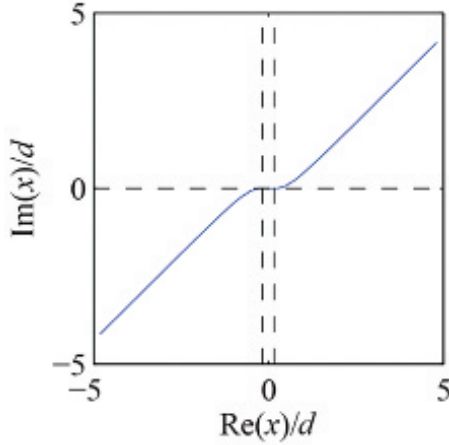


Fig. 1.7. The considered contour in the complex plane.

At $x' \in (-e/2, e/2)$ the contour lies on the real axis, away from the real axis $x'' \rightarrow \pm\infty$ and the imaginary part x' also tends to infinity, with the condition $x'x'' > 0$. This selection of the contour provides decay of the electromagnetic field with increasing distance from the real axis. To introduce artificial periodization, consider the transformation of coordinates $F(\tilde{x}) = x$ mapping the contour on the complex plane into the interval $\tilde{x} \in (-d/2, d/2)$ where \tilde{x} is a new real coordinate. At the same time at $\tilde{x} \in (-e/2, e/2)$ the field will be the same as the solution of the original equation (1.159), while at $\tilde{x} \rightarrow \pm d/2$ the field components will tend to zero by the choice of the contour in the complex plane x . To move from equation (1.159) to a new differential equations depending on a variable \tilde{x} , we need to make the following change of the differential operator: $\partial/\partial x \rightarrow f \cdot \partial/\partial \tilde{x}$ where $f(\tilde{x}) = d\tilde{x}/dx = (dF(\tilde{x})/d\tilde{x})^{-1}$. As a result, we obtain the differential equation

$$\frac{\partial^2 H_y}{\partial z^2} + \varepsilon(x) f \frac{\partial}{\partial \tilde{x}} \left[\frac{f}{\varepsilon(x)} \frac{\partial H_y}{\partial \tilde{x}} \right] + k_0^2 \varepsilon(x) H_y = 0. \quad (1.161)$$

Equation (1.161) can be solved by the Fourier modal method since the task now allows artificial periodization (since the field at the boundaries of the period $\tilde{x} = \pm d/2$ tends to zero). Using the

expansions (1.27), the solution of the differential equation (1.161), which describes a general representation of the field in the layer can be reduced to a system of differential equations

$$\frac{d}{dz'} \begin{bmatrix} \mathbf{U}_y \\ \mathbf{S}_x \end{bmatrix} = - \begin{bmatrix} \mathbf{0} & \mathbf{E}^* \\ \mathbf{F}_x \mathbf{K}_x \mathbf{E}^{-1} \mathbf{F}_x \mathbf{K}_x - \mathbf{I} & \mathbf{0} \end{bmatrix} \begin{bmatrix} \mathbf{U}_y \\ \mathbf{S}_x \end{bmatrix}, \quad (1.162)$$

where $z' = k_0 z$, \mathbf{F}_x is the Toeplitz matrix formed from the coefficients of expansion of the function f into the Fourier series. Comparing the second system of differential equations (1.48) with (1.162), one can see that the latter is derived from the first formal change $\mathbf{K}_x \rightarrow \mathbf{F}_x \mathbf{K}_x$. Note that in the general case, when the field in the layer is described by a system of differential equations (1.35) with the matrix (1.36), the perfectly matched absorbing layers can be introduced using the same formal change.

We now give as an example the type of function $f(\tilde{x})$ that describes the coordinate transformation [23]:

$$f(\tilde{x}) = \begin{cases} 1, & |\tilde{x}| < e/2, \\ \left[1 - \gamma \sin^2 \left(\pi \frac{|\tilde{x}| - e/2}{q} \right) \right] \cos^2 \left(\pi \frac{|\tilde{x}| - e/2}{q} \right), & \frac{e}{2} < |\tilde{x}| < \frac{d}{2}, \end{cases} \quad (1.163)$$

where $q = d - e$ is the total size of the region corresponding to the absorbing layers, γ is a complex parameter characterizing the absorbing layer (typical value $\gamma = 1/(1-i)$). For this function, the coefficients of the Fourier series can be found analytically and have the form

$$f_n = \delta_{n0} - \frac{q}{2d} (-1)^n \left[\left(1 + \frac{\gamma}{4} \right) \operatorname{sinc} \left(\frac{nq}{d} \right) + \frac{1}{2} \operatorname{sinc} \left(\frac{nq}{d} - 1 \right) + \frac{1}{2} \operatorname{sinc} \left(\frac{nq}{d} + 1 \right) - \frac{\gamma}{8} \operatorname{sinc} \left(\frac{nq}{d} - 2 \right) - \frac{\gamma}{8} \operatorname{sinc} \left(\frac{nq}{d} + 2 \right) \right], \quad (1.164)$$

where δ_{n0} is the Kronecker symbol, $\operatorname{sinc}(x) = \sin(\pi x)/(\pi x)$. We note that the function $f(\tilde{x})$ corresponds to the contour in the complex plane

$$F(\tilde{x}) = \left\{ \begin{array}{l} x, |\tilde{x}| < e/2, \\ \tilde{x} \left[\frac{e}{2} + \frac{q}{\pi(1-\gamma)} \left\{ \begin{array}{l} \operatorname{tg} \left(\pi \frac{|\tilde{x}| - e/2}{q} \right) \\ - \frac{\gamma}{\sqrt{1-\gamma}} \operatorname{arctg} \left[\sqrt{1-\gamma} \operatorname{tg} \left(\pi \frac{|\tilde{x}| - e/2}{q} \right) \right] \end{array} \right\} \right] \right\}, \\ \frac{e}{2} < |\tilde{x}| < \frac{d}{2}. \end{array} \right. \quad (1.165)$$

The real and imaginary parts of the function $f(\tilde{x})$ at $e = d/3$, $\gamma = 1/(1-i)$ are shown in Fig. 1.8, the contour in the complex plane is shown in Fig. 1.7.

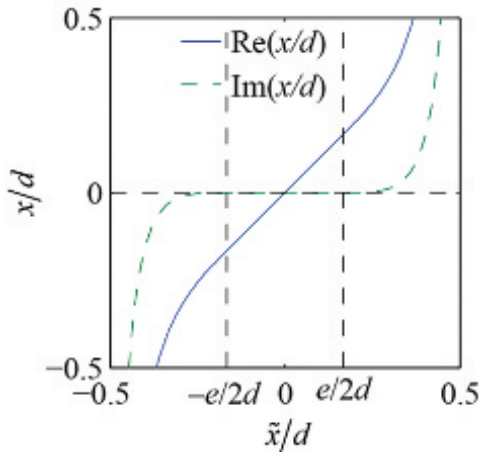


Fig. 1.8. The real and imaginary parts of the contour in the complex plane, depending on the value of the new real variable.

1.1.4.3. Solution of the diffraction problem

Stages of solving the diffraction problem in this case coincide with the stages of solving the diffraction problem of a plane wave on a two-dimensional diffraction structure described in subsection 1.2. The differences lie in the form of the field above and below the structure (in regions 1 and 3 in Fig. 1.5). Since the regions above and below the structure in this case are not uniform, the electromagnetic field therein can not be represented in the form of Rayleigh expansions (1.20) and (1.21). Representation of the field in these areas can be obtained similarly to the representation of the field in the layer of

the structure obtained by solving a system of differential equations of the form (1.35) (with the possible modification of the matrix of the system by introducing perfectly matched layers in the form of coordinate transformations). Thus, the field above and below the structure will be presented in the form of the Fourier series (1.27) and the expressions for the x - and y -Fourier components of the fields will be similar to (1.58):

$$\begin{bmatrix} \mathbf{S}_y^U \\ \mathbf{S}_x^U \\ \mathbf{U}_y^U \\ \mathbf{U}_x^U \end{bmatrix} = \mathbf{W}_{inc} \exp(\lambda_{inc} k_0 z) A_{inc} + \mathbf{W}_U^{(-)} \exp(\Lambda_U^{(-)} k_0 z) \mathbf{R}, \quad (1.166)$$

$$\begin{bmatrix} \mathbf{S}_y^D \\ \mathbf{S}_x^D \\ \mathbf{U}_y^D \\ \mathbf{U}_x^D \end{bmatrix} = \mathbf{W}_D^{(+)} \exp[\Lambda_D^{(+)} k_0 (z - z_L)] \mathbf{T}. \quad (1.167)$$

Similarly to the expressions (1.20), (1.21), the indices U and D correspond to the regions above and below the structure (reas 1 and 3 in Fig. 1.5). The first term in (1.166) describes the incident wave with an amplitude A_{inc} , with its eigenvalue λ_{inc} selected from $\Lambda_U^{(+)}$ as closest one to the propagation constant of the incident mode calculated by solving the corresponding dispersion equation.

The system of linear equations (1.71), which describes the condition of equality of the tangential components of the electromagnetic field at the boundaries of layers of the structure, retains its form, however, the expressions for \mathbf{D} , $\mathbf{P}^{(U)}$ and $\mathbf{P}^{(D)}$, included in the equation, change. In this case,

$$\begin{aligned} \mathbf{D} &= \mathbf{W}_{inc} A_{inc}, \\ \mathbf{P}^{(U)} &= \mathbf{W}_U^{(-)}, \\ \mathbf{P}^{(D)} &= \mathbf{W}_D^{(+)}. \end{aligned} \quad (1.168)$$

As before, for obtaining a numerically-stable solution of equations (1.71) and finding the amplitudes of the transmitted and reflected waves we can use the scattering matrix algorithm, described in section 1.2.6. For the calculation of the distribution of the field we can use a stable procedure described in subsection 1.2.7.

1.1.4.4 The energy characteristics of the reflected and transmitted light

First we find the energy characteristics of the transmitted radiation. To do this, we calculate the flux of the z -component of the Umov–Poynting vector $S_z = \text{Re}(E_x H_y^* - E_y H_x^*)/2$ of the transmitted waves within a period through the segment $z = z_L$. We rewrite the representation of the field (1.167) for $z = z_L$, separating parts of the eigenvectors $\mathbf{W}_D^{(+)}$ corresponding to the various components of the electromagnetic field:

$$\begin{bmatrix} \mathbf{S}_y^D \\ \mathbf{S}_x^D \\ \mathbf{U}_y^D \\ \mathbf{U}_x^D \end{bmatrix} = \begin{bmatrix} \mathbf{W}_{D,S_y}^{(+)} \\ \mathbf{W}_{D,S_x}^{(+)} \\ \mathbf{W}_{D,U_y}^{(+)} \\ \mathbf{W}_{D,U_x}^{(+)} \end{bmatrix} \mathbf{T}. \quad (1.169)$$

Taking into account (1.169) in (1.27) and assuming for the sake of simplicity that $y = 0$, we obtain:

$$\begin{cases} E_x = \sum_k t_k \sum_j w_{j,k,S_x} \exp(ik_{x,j}x), \\ E_y = \sum_k t_k \sum_j w_{j,k,S_y} \exp(ik_{x,j}x), \\ H_x = -i \sum_k t_k \sum_j w_{j,k,U_x} \exp(ik_{x,j}x), \\ H_y = -i \sum_k t_k \sum_j w_{j,k,U_y} \exp(ik_{x,j}x), \end{cases} \quad (1.170)$$

where t_i are the elements of the vector \mathbf{T} , $w_{j,i,S_x}, w_{j,i,S_y}, w_{j,i,U_x}$, and w_{j,i,U_y} are the elements of vectors $\mathbf{W}_{D,S_x}^{(+)}, \mathbf{W}_{D,S_y}^{(+)}, \mathbf{W}_{D,U_x}^{(+)}$, and $\mathbf{W}_{D,U_y}^{(+)}$ respectively. Taking into account (1.170) in the expression for the z -component of the Umov–Poynting vector, we get:

$$S_d^D = 2 \int_0^d S_z dx = \sum_{k,m,j,n} \int_0^d \text{Re} \left(\frac{it_k t_m^* \left[w_{j,k,S_x} w_{n,m,U_y}^* - w_{j,k,S_y} w_{n,m,U_x}^* \right]}{\exp \left[i(k_{x,j} - k_{x,n})x \right]} \right) dx. \quad (1.171)$$

Given the equality $\int_0^d \text{Re} \left(a \exp \left[i(k_{x,j} - k_{x,n})x \right] \right) dx = \text{Re}(a) d \delta_{jn}$ from (1.171) we obtain:

$$S_d^D = d \sum_{k,m} \text{Im} \left(t_k t_m^* \sum_j \left[w_{j,k,S_y} w_{j,m,U_x}^* - w_{j,k,S_x} w_{j,m,U_y}^* \right] \right). \quad (1.172)$$

From (1.172) it follows that, in contrast to the above-mentioned periodic structures, the flux of the Umov–Poynting vector in the period can not be represented as a sum of terms, each of which corresponds to a single wave. Note, however, that the waveguide and plasmonic modes, propagating in the original structure, the following condition of orthogonality is numerically satisfied (up to the order of 10^{-10}):

$$\sum_j \left[w_{j,k,S_y} w_{j,m,U_x}^* - w_{j,k,S_x} w_{j,m,U_y}^* \right] = 0, \quad k \neq m, \quad (1.173)$$

where k is a fixed number, and m runs through all values from 1 to the number of waves corresponding to the dimensionality of the system of differential equations (1.35). Verification of fulfillment of this condition allows us to judge the correctness of the choice of the values of the period d for artificial periodization and the parameters of absorbing layers. But the waves, for which the orthogonality condition (1.173) is fulfilled, can be given the energy characteristics similar to the intensity of the diffraction orders and determined by expression

$$I_n^T = \frac{|t_n|^2 \left| \text{Im} \left(\sum_j \left[w_{j,n,S_y} w_{j,n,U_x}^* - w_{j,n,S_x} w_{j,n,U_y}^* \right] \right) \right|}{|A_{inc}|^2 \left| \text{Im} \left(\sum_j \left[w_{j,inc,S_y} w_{j,inc,U_x}^* - w_{j,inc,S_x} w_{j,inc,U_y}^* \right] \right) \right|}, \quad (1.174)$$

where $w_{j,inc,S_x}, w_{j,inc,S_y}, w_{j,inc,U_x}$, and w_{j,inc,U_y} are the elements of the vector \mathbf{W}_{inc} . The denominator of (1.174) gives the flux of the Umov–Poynting vector of the incident wave. Similarly, the energy characteristics of the reflected waves are calculated: the elements of the vector \mathbf{T} (1.174) are replaced by the elements of the vector \mathbf{R} , and the elements of the eigenvectors from the matrix $\mathbf{W}_D^{(+)}$ are replaced by the corresponding values from the matrix $\mathbf{W}_D^{(-)}$.

1.1.4.5. Numerical example

Consider as an example the propagation of a TM-polarized

fundamental mode of the plane-parallel waveguide through a couple of grooves in it (Fig. 1.9) [21]. The refractive indices of the materials are shown in the Fig., the waveguide thickness is 300 nm, the width of the grooves and the step separating them are 150 nm. The wavelength of the radiation in free space is 975 nm.

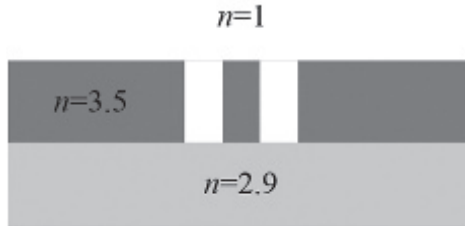


Fig. 1.9. The geometry of the diffraction problem.

Table 1.1 shows the values of the coefficients of reflection and transmission (energy characteristics of the reflected and transmitted modes) depending on the number of harmonics N (the total number of harmonics is $2N + 1$). Simulation was carried out using perfectly matched absorbing layers in the form of coordinate transformations. The following simulation parameters were: $e = 900$ nm, $d = 3e$, $\gamma = 1/(1-i)$, the middle of the waveguide coincided with the middle of the period.

Table 1.1. Coefficients of reflection and transmission for the TM-polarized fundamental mode

N	I^R	I^T
50	0.356216	0.129970
100	0.355637	0.129675
150	0.355569	0.129619
200	0.355531	0.129604

1.2. Methods for calculating eigenmodes of periodic diffractive structures

1.2.1. Calculation of modes based on the calculation of the poles of the scattering matrix

The diffractive micro- and nanostructures with the resonant properties are of great interest for designing of modern elements of integrated optics and photonics [19,24–31]. The resonant properties are manifested in the abrupt change in the transmission and reflection spectra, and are usually associated with the excitation of the